Contrib Mineral Petrol (2012) 163:745–768
DOI 10.1007/s00410-011-0697-1

ORIGINAL PAPER

Li isotopes and trace elements as a petrogenetic tracer in zircon: insights from Archean TTGs and sanukitoids

Anne-Sophie Bouvier · Takayuki Ushikubo · Noriko T. Kita · Aaron J. Cavosie · Reinhard Kozdon · John W. Valley

Received: 7 March 2011 / Accepted: 14 September 2011 / Published online: 2 October 2011

Abstract We report δ^7Li, Li abundance ([Li]), and other trace elements measured by ion probe in igneous zircons from TTG (tonalite, trondhjemite, and granodiorite) and sanukitoid plutons from the Superior Province (Canada) in order to characterize Li in zircons from typical Archean continental crust. These data are compared with detrital zircons from the Jack Hills (Western Australia) with U–Pb ages greater than 3.9 Ga for which parent rock type is not known. Most of the TTG and sanukitoid zircon domains preserve typical igneous REE patterns and CL zoning. [Li] ranges from 0.5 to 79 ppm, typical of [Li] in continental zircons. Atomic ratios of (Y + REE)/(Li + P) average 1.0 ± 0.7 (2SD) for zircons with magmatic composition preserved, supporting the hypothesis that Li is interstitial and charge compensates substitution of trivalent cations. This substitution results in a relatively slow rate of Li diffusion. The δ^7Li and trace element data constrain the genesis of TTGs and sanukitoids. [Li] in zircons from granitoids is significantly higher than from zircons in primitive magmas in oceanic crust. TTG zircons have δ^7Li (3 ± 8‰) and δ^{18}O in the range of primitive mantle-derived magmas. Sanukitoid zircons have average δ^7Li (7 ± 8‰) and δ^{18}O higher than those of TTGs supporting genesis by melting of fluid-metasomatized mantle wedge. The Li systematics in sanukitoid and TTG zircons indicate that high [Li] in pre-3.9-Ga Jack Hills detrital zircons is a primary igneous composition and suggests the growth in proto-continental crust in magmas similar to Archean granitoids.

Keywords Zircon · Trace elements · Lithium isotopes · SIMS · Jack Hills · TTG · Sanukitoid

Communicated by F. Poitrasson.

Electronic supplementary material The online version of this article (doi:10.1007/s00410-011-0697-1) contains supplementary material, which is available to authorized users.

A.-S. Bouvier (✉) · T. Ushikubo · N. T. Kita · R. Kozdon · J. W. Valley
WiscSIMS, Department of Geoscience, University of Wisconsin, Madison, WI 53706, USA
e-mail: anne-sophie.bouvier@nrm.se

Present Address:
A.-S. Bouvier
Swedish Museum of Natural History, 10405 Stockholm, Sweden

A. J. Cavosie
Department of Geology, University of Puerto Rico, Mayagüez, PR 00681, USA

Introduction

Zircons are a retentive accessory mineral in many rocks. They are extensively used for U–Pb geochronology, giving useful information about tectonic events and related processes (e.g., Davis et al. 2003). Zircons also give valuable geochemical information from oxygen isotope ratios and trace elements (Hoskin and Schaltegger 2003; Valley 2003). Magmatic δ^{18}O values are generally preserved in non-metamict zircons, even through high-grade metamorphism and anatexis (Page et al. 2007; Valley et al. 2005; Watson and Cherniak 1997). Grimes et al. (2007) used trace elements to show that zircons from continental crust can be distinguished from oceanic crust. Recently, Li content ([Li]) and δ^7Li in zircons have been reported (Grimes et al. 2011; Li et al. 2011; Ushikubo et al. 2008) showing that Li is useful for characterizing a zircon's parent rock. However, interpreting the significance of [Li] and δ^7Li in zircons requires better understanding of the

possible effects of alteration in Li and δ^7Li distribution in zircon, Li substitution mechanisms, and Li diffusion rates in zircon.

Here, we report the analysis of δ^7Li, [Li], and other trace elements in zircons coupled to imaging for well-studied igneous suites. This is the first study reporting analyses of δ^7Li, associated with 23 trace elements (Li, P, Ca, Ti, V, Fe, Y, REE, U, and Th) in single analysis pits in zircon. Due to intracrystalline zoning, such correlated analyses are necessary to test the proposed Li substitutions in zircons.

We chose igneous zircons from TTGs and sanukitoids with ages ranging from 2.7 to 3.0 Ga, which are typical Archean granitoids (e.g., King et al. 1998). The selected TTG and sanukitoid zircons are from the Superior Province (Canada), and δ^{18}O(Zrc) and U–Pb ages are reported elsewhere (Davis et al. 2005; King et al. 1998). The use of well-described zircons with known parent rocks allows testing the potential of [Li] and δ^7Li as petrogenetic tracers. The differences in trace elements, Li, and δ^7Li between zircons from four TTG and four sanukitoid plutons are discussed in terms of their different petrogenesis. These data are also compared to Archean detrital zircons from the Jack Hills (Western Australia) that are older than 3.9 Ga (up to 4.35 Ga) and for which parent rock type is uncertain.

Li substitution in zircons

While Li is a mobile element in many processes, zircon appears to be highly retentive (Ushikubo et al. 2008); however, Li exchange in zircon is not well understood. The mechanism of lithium substitution in zircon affects chemical diffusion rates and must be evaluated before it can be interpreted as reflecting magmatic compositions. Zircon is an orthosilicate in which isolated SiO_4 tetrahedra shares corners and edges with distorted ZrO_8 polyhedra. The zircon crystal structure incorporates a wide range of trace elements, including Li, P, Y, Ti, Hf, U, Th, and REE (Finch et al. 2001; Hanchar et al. 2001; Hoskin and Schaltegger 2003). Incorporation of REE in zircon is commonly assumed to be a "xenotime-type" substitution, because of the high [P] in many zircons and because zircon is isostructural with xenotime (YPO_4). The charge-balanced substitution is as follows:

$$(Y + REE)^{3+} + P^{5+} = Zr^{4+} + Si^{4+} \quad (1)$$

If xenotime-type substitution solely governs the REE incorporation in zircons, P^{5+} and REE^{3+} compensate and $[(Y + REE)/P]_{atomic}$ should be 1. However, numerous studies have observed an excess of total REE compared with P (i.e., $[(Y + REE)/P]_{atomic} > 1$), indicating that at least one other substitutional mechanism occurs (Cavosie et al. 2006; Hinton and Upton 1991; Pidgeon et al. 1998; Speer 1982). Possible substitutions are summarized in Table 1. Some substitutions are simple, such as tetravalent Hf, U, Th, Ti, and Sn ions that could directly substitute for Zr^{+4}, whereas other elements require a coupled substitution for charge balance. Finch et al. (2001) and Hanchar et al. (2001) suggested that Li substitutes on an interstitial site, charge-balancing REE and Y (see Table 1), leading to a couple substitution as follows:

$$Li^{1+}_{(interstitial)} + (Y + REE)^{3+} = Zr^{4+} + \square_{(interstitial)} \quad (2)$$

When converted to atomic proportions, each ppm of Li (at. wt $\sim$ 7 amu) compensates for over twenty times its weight in REE (at. wt $\sim$ 150 amu) in Eq. (2). In this case, if Li and P compensate REE, the ratio defining these two coupled substitutions, $[(Y + REE)/(Li + P)]_{atomic}$, should be 1 (Ushikubo et al. 2008). Because $^{IV}Li^{1+}$ has a larger ionic radius than Si^{4+} (Shannon 1976), Li is unlikely to be incorporated in Si sites. Alternatively, ^{VIII}Li could fit ^{VIII}Zr sites, associated with 3 interstitial Li for charge compensation (Eq. 3). Li could also be 100% interstitial for charge compensation of Zr, if an eightfold vacancy can exist (Eq. 4).

$$^{VIII}Li^{+} + 3Li^{+}_{(intersitial)} = ^{VIII}Zr^{4+} + 3\square_{(interstitial)} \quad (3)$$

$$4Li^{+}_{(interstitial)} + ^{VIII}\square = Zr^{4+} + 4\square_{(interstitial)} \quad (4)$$

Li substitution in natural zircons was recently discovered to vary by over 5 orders of magnitude, from <2 ppb to 250 ppm (Ushikubo et al. 2008). Zircons from primitive magmas, the mantle, and ocean crust are low in [Li] (kimberlite megacrysts <2 ppb, mid-ocean ridge gabbro <10 ppb, and mid-ocean ridge plagiogranite < 100 ppb), whereas zircons from continental crust have significantly higher Li contents (typically 1–100 ppm, Barth and Wooden 2010; Grimes et al. 2011; Ushikubo et al. 2008).

Li isotopic fractionation

Fresh igneous rocks from the mantle have δ^7Li(whole rock) = 3.8 ± 1.5‰ (Chan et al. 2002a, b; Jeffcoate et al. 2007; Magna et al. 2006; Seitz et al. 2004; Tomascak et al. 2008), whereas seawater has very high δ^7Li ($\sim$31‰; Chan and Edmond 1988; Millot et al. 2004; Tomascak 2004; You and Chan 1996). Li isotope fractionation during fluid–rock interaction causes up to 50‰ variation in δ^7Li, with products of subaerial weathering as low as −20‰ (Chan and Edmond 1988; Chan et al. 1992, 2002a; Pistiner and Henderson 2003; Rudnick and Ionov 2007; Seyfried et al. 1998; Teng et al. 2008). Continental crust has an average δ^7Li(WR) of +1.7‰ (Teng et al. 2009), making δ^7Li a potential tracer of continental alteration and weathering.

Table 1 Substitution in zircons

Element	Equations	References
	Xenotime substitution	
Y^{3+}	$(Y + REE)^{3+} + P^{5+} = Zr^{4+} + Si^{4+}$	
	Simple substitutions	
$(OH)_4$	$(OH)_4 = SiO_4$	Frondel (1953)
Hf^{4+}	$Hf^{4+} = Zr^{4+}$	Frondel (1953)
U^{4+}, Th^{4+}, Ti^{4+}, Sn^{4+}	$(U, Th, Ti, Sn)^{4+} = Zr^{4+}$	Frondel (1953)
	Coupled substitutions	
Li^{+}	$Li^{1+}_{(interstitial)} + REE^{3+} = Zr^{4+}$	Finch et al. (2001), Hanchar et al. (2001)
$(OH)^{-}$	$M^{n+} + n(OH)^{-} + (4 - n)H_2O = Zr^{4+} + (SiO_4)^{4-}$ [a]	Caruba and Iacconi (1983)
Mg^{2+}, Fe^{2+}	$(Mg,\ Fe)^{2+}_{(interstitial)} + 3(Y, REE)^{3+} + P^{5+} = 3Zr^{4+} + Si^{4+}$	Hoskin et al. (2000)
Al^{3+}, Fe^{3+}	$(Al,\ Fe)^{3+}_{(interstitial)} + 4(Y, REE)^{3+} + P^{5+} = 4Zr^{4+} + Si^{4+}$	Hoskin et al. (2000)
S^{6+}	$S^{6+} + 2(Y + REE)^{3+} = Si^{4+} + 2Zr^{4+}$	Based on Romans et al. (1975)
Ca^{2+}	$Ca^{2+}_{(interstital)} + 2(Y + REE)^{3+} = 2Zr^{4+}$	Based on Romans et al. (1975)
Sc^{3+}	$Sc^{3+} + P^{5+} = Zr^{4+} + Si^{4+}$	Halden et al. (1993)
Zr^{4+}	$Zr^{4+}_{(interstitial)} + 4REE^{3+} = 4Zr^{4+}$	Finch et al. (2001)
Nb^{5+}, Ta^{5+}	$(Y + REE)^{3+} + (Nb, Ta)^{5+} = 2Zr^{4+}$	Es'kova (1959)
Mo^{6+}	$Mo^{6+} + 2REE^{3+} = Si^{4+} + 2Zr^{4+}$	Speer (1982)
	$Mo^{6+} + 2REE^{3+} = 3Zr^{4+}$	Speer (1982)
	$Mo^{6+}_{(intersitital)} + 6REE^{3+} = 6Zr^{4+}$	Finch et al. (2001)

a *M* metal cation, *n* integer

Lithium isotopes can also be fractionated by kinetic processes of chemical diffusion in silicate melts and hydrothermal fluids, or fluid-assisted grain-boundary diffusion, where ^{6}Li diffuses faster than ^{7}Li (Lundstrom et al. 2005; Richter et al. 2003; Teng et al. 2006a). Diffusion processes can produce low values of $\delta^{7}Li$ over restricted distances and time-scales, but only if there is an initial gradient in [Li]. The resulting low $\delta^{7}Li$ will be in the initially Li-poor phase. In minerals, the diffusion coefficient varies depending on faster or slower pathways within the crystal lattice, which may include eightfold versus interstitial sites, crystal defects, and radiation damage (Cherniak and Watson 2010; Dohmen et al. 2010; Watson and Baxter 2007; Watson and Cherniak 1997; Zhang et al. 2006). Recently, two studies investigated Li diffusion in minerals: Dohmen et al. (2010) experimentally calibrated the diffusion rate of Li in olivine, and Cherniak and Watson (2010) determined that the diffusion rate of Li in zircon is slower than in olivine but did not specify the substitution mechanism of Li in their experimental zircon. Cherniak and Watson (2010) conclude that Li diffusion is relatively insensitive to crystal orientation and the presence of hydrous species, that Li in an interstitial site may diffuse faster than if in eightfold coordination, that Li diffusion rate in zircon is faster than other cations (e.g., Dy, Hf, and Pb), and that Li isotope ratio in zircon will re-equilibrate under medium- or high-temperature regional metamorphism. The authors calculated that a 100-μm-diameter zircon could retain Li composition at its center for up to 1.5 Ga at 450°C. They also calculated Li diffusive exchange during cooling. Typical size zircons could retain Li compositions in the center of grains during slow cooling (1–2°C/Ma) for maximum temperatures up to 500°C, whereas at 750°C, they would retain core composition only if cooling is fast (>10^{4}°C/Ma). Cherniak and Watson (2010) have shown that Li tracer diffusion is faster than REEs but do not evaluate the effect of REE substitution on Li diffusion in their experimental zircon. Li-coupled substitutions in olivine are different from those in zircon, so diffusivity should not be expected to be similar. If Li is mostly interstitial in zircons (Eq. 2), and Li^{+1} is charge balanced by REE^{+3}, it cannot vary independently, and thus its rate of chemical diffusion depends on the REE diffusivity, which is much slower than that proposed by Cherniak and Watson (2010) (e.g., $D(Sm) = 2.9 \times 10^{8}\exp(-841 \pm 57\ kJ\ mol^{-1}/RT)\ m^{2}\ s^{-1}$; Cherniak et al. 1997; Cherniak and Watson 2003). Under these conditions, chemical diffusion of Li will be exceedingly slow even during granulite facies metamorphism and anatexis, as is shown by preserved [Li] zoning in zircons from migmatites in the Adirondack Mountains and Kapuskasing Uplift (Ushikubo et al. 2008; Bowman et al. 2011). Thus, large Li

isotope fractionations accompanying chemical diffusion will not occur in zircon. Primary magmatic δ^7Li values should be retained and provide valuable information if tracer diffusion of Li is also sufficiently slow.

Rates of isotope exchange by tracer diffusion may be faster than chemical diffusion. However, the boundary conditions for this process are different than those of chemical diffusion. Low values of δ^7Li will only result if caused by equilibrium fractionation or by mixing with an even lower δ^7Li phase.

Zircon background

Type-1 (primary) and Type-2 (secondary) zircon domains

Two types of normalized REE patterns were recognized in zircons by Cavosie et al. (2006). Type-1 domains have typical REE patterns (e.g., large enrichment in HREE compared with chondrite) and marked positive Ce and negative Eu anomalies. They are usually thought to be representative of original magmatic values. In contrast to Type-1 domains, Type-2 domains are characterized by higher LREE concentrations and a flatter LREE profile, with $La_N > 1$, $Pr_N > 10$, and $Sm_N/La_N < 10$. Type-2 zircon domains have been reported for different locations and are suggested to be non-representative of any parent magma (Cavosie et al. 2006; Hoskin 2005; Whitehouse and Kamber 2003). Thus, the genesis of these domains must be considered before further interpretation of these data. Type-2 domains have been attributed to various post-magmatic processes, including new mineral growth during hydrothermal events and alteration in originally igneous zircons. Whitehouse and Kamber (2003) suggest that LREE enrichment in Greenland zircons (>3.8-Ga cores and ca. 3.65-Ga rims) could be due to re-crystallization of zircon, erasing original igneous oscillatory zoning and mobilizing more incompatible trace elements (i.e., LREE, Th, and U) into the re-crystallized zones behind a re-crystallization front. Likewise, Hoskin (2005) suggests that the Type-2 Jack Hills domains represent "hydrothermal zircons" that formed from a LREE-bearing, high δ^{18}O ($\geq$6–10‰) fluid. In contrast, Cavosie et al. (2006) show that some Type-2 ion microprobe analyses in Jack Hills zircons encountered hidden mineral inclusions, including phosphates, and are thus not true zircon compositions. They further propose that when no mineral inclusion is encountered, the Type-2 LREE enrichment results from radiation damage or alteration in pre-existing igneous zircons, possibly at a very low fluid/rock ratio, since no anomalous δ^{18}O values were found in Type-2 domains. Thus, non-porous Type-2 zircons should not be assumed to have precipitated from a hydrothermal fluid, as hydrothermally precipitated zircon would likely produce measurable variations in δ^{18}O [see also discussion in Cavosie et al. (2009)], which are not observed in Jack Hills zircons.

Effects of radiation damage on trace element compositions

Radiation damage increases the susceptibility of zircon to elemental exchange and alteration (e.g., Geisler and Schleicher 2000a; Silver and Deutsch 1963; Utsunomiya et al. 2007). Geisler et al. (2003a) demonstrated that alteration can lower the Zr, Si, Hf, REE, U, Th, Th/U, and radiogenic Pb contents of zircons and increase the concentration of other cations (Ca^{2+}, Ba^{2+}, Mg^{2+}, and Al^{3+}). Utsunomiya et al. (2007) studied radiation-damaged zircons from a 3.3-Ga granite adjacent to the Jack Hills metasedimentary belt in order to examine the effects of radiation damage as a function of dose. In spite of very high doses within localized domains ($0.21–1.0 \times 10^{17}$ α-decay events/mg), damage is partially annealed and none of the zircons are fully amorphous. Ca and P contents correlate with dose, ranging up to $\sim$4,000 and 25,000 ppm, respectively, in the most altered domains. A number of studies have shown that an increase in [Ca] in zircons is correlated with higher α-decay doses, suggesting late hydration of the radiation-damaged (higher [U] and [Th]) areas (Aines and Rossman 1986; Geisler et al. 2003b; Geisler and Schleicher 2000b; Rayner et al. 2005; Utsunomiya et al. 2007; Woodhead et al. 1991). The effects of radiation damage on [Li] and δ^7Li are not known.

Samples

Sanukitoid and TTG samples

The Superior Province (Canada), the largest exposed Archean craton, is thought to be a series of island arcs (granite-greenstone belts) and fore-arc accretionary prisms (metasedimentary belts) accreted onto an older craton (Williams et al. 1991). Zircons from TTG (tonalite, trondhjemite, and granodiorite) and from sanukitoid plutons were chosen to represent Archean granitoids from the western Superior Province (e.g., Davis et al. 2005; King et al. 1998).

TTG samples

Archean TTGs are silica-rich granitoids (>63 wt%) with high Na_2O contents (3–7 wt%), Al_2O_3 contents > 15% at 70 wt% SiO_2, Sr > 300 ppm, Y < 20 ppm, Yb < 1.8 ppm, Nb $\leq$ 10 ppm, and low-Mg amphibole (Barker 1979; Condie 2005; Drummond and Defant 1990; Martin et al.

2005) and are depleted in HREE (Beakhouse and McNutt 1991). The chemical compositions of TTGs suggest that they are derived from melting of hydrated subducted tholeiitic crust or hydrous basaltic material at the base of thickened crust (e.g., Huang et al. 2010; Martin et al. 2005; Smithies 2000; Xiong et al. 2009).

The TTG plutons from the western Superior Province intruded pre- to syn-Kenoran Orogeny (2.67–3.0 Ga; see Davis et al. 2005 for a review). TTG zircons analyzed here come from two diorites (DD81-32 and C88-29) and two tonalites (C92-30 and DD86-25a). Diorite DD81-32 and tonalite DD86-25a are from the Wabigoon sub-province, whereas diorite C88-29 and tonalite C92-30 come from English River and Wawa sub-provinces, respectively (Fig. 2; Table 5 in King et al. 1998). C92-30 and DD86-25a have 64.9 and 68.9 wt% SiO_2, respectively (King et al. 1998). Zircons from the four rocks yield ages ranging from 2.70 to 2.73 Ga and average $\delta^{18}O(Zrc) = 5.5 \pm 0.8‰$ (2SD) (King et al. 1998). The $\delta^{18}O$ values (measured by laser fluorination in the 2-mg bulk concentrates) for the four rocks of this study vary from 5.52 to 6.47‰, averaging 5.8‰, close to values of zircons from mid-ocean ridge gabbros and plagiogranites or other primitive magmas ($5.3 \pm 0.6‰$; Cavosie et al. 2009; Grimes et al. 2011; Valley et al. 1998, 2005).

Sanukitoid samples

Sanukitoids are plutonic granitoids characterized by SiO_2 from 55 to ~60 wt% for the less-evolved magmas (up to 70 wt% for the more-evolved magmas), $K_2O > 1$wt%, Mg # > 0.60, Ni and Cr both >100 ppm, both Sr and Ba > 1,000 ppm and LREE > 100 times chondritic values, and without a Eu anomaly (Shirey and Hanson 1984). Most authors agree that these plutons are derived from melting of metasomatized mantle wedge, followed by fractional crystallization in the crust, but amounts of crustal contamination and the nature of the metasomatizing fluids are uncertain (Moyen et al. 1997; Shirey and Hanson 1984; Smithies and Champion 1999; Stern 1989; Stern and Hanson 1991; Stevenson et al. 1999, 2009).

The western Superior Province sanukitoid samples are syn- to post-tectonic, chemically enriched plutons (2.68–2.70 Ga; $\delta^{18}O(Zrc) = 6.37 \pm 0.48‰$, see King et al. 1998; Davis et al. 2005 for a review). We chose zircons from four monzodiorites (DD96-4, DD96-8, and DD96-10 from Wabigoon and C92-31 from Wawa sub-provinces), with SiO_2 ranging from 57.2 to 62.7 wt%. The ages of the four monzodiorites range from 2.68 to 2.70 Ga, and their zircons display a small $\delta^{18}O(Zrc)$ range (6.09–6.46‰) measured in bulk 2-mg samples by laser fluorination (King et al. 1998). The values of $\delta^{18}O(Zrc)$ in these sanukitoids average $6.28 \pm 0.36‰$ and are mildly elevated relative to zircons in high-temperature equilibrium with MORB, TTG, and other primitive magmas, indicating input from a higher $\delta^{18}O$ supracrustal source (dehydration fluid from subducted oceanic crust, melt of subducted sediments, or continental crust).

Jack Hills zircons

We chose detrital zircon grains from the Jack Hills metaconglomerate (Western Australia) (samples 01JH13 and 01JH54) that were all previously analyzed for U–Pb age, [Li], and oxygen and lithium isotope ratios (Cavosie et al. 2004, 2005; Ushikubo et al. 2008). Some zircons were also analyzed for trace elements (Cavosie et al. 2006); however, the trace element analyses were made in different sessions and cannot be perfectly correlated because they are not all from single pits. These zircons are dominantly concordant in U–Pb age, suggesting that the dated domains preserved magmatic compositions of U, Th, Pb, trace elements, and $\delta^{18}O$. Twenty-five dated zircons are older than 3.9 Ga (up 4.35 Ga) and three are from 3.36 to 3.90 Ga. They show growth zoning by CL, and their average $\delta^{18}O$ values range from 4.6 to 7.3‰, with one at 8.5‰ (Cavosie et al. 2005; Ushikubo et al. 2008). The Li content and Li isotope ratio of the zircons used for this study range from $\delta^{7}Li = -18.4$ to +11.8‰ and [Li] = 1.2–70.7 ppm (Ushikubo et al. 2008).

Analytical methods

Trace elements

Before analysis, zircons were imaged by cathodoluminescence (CL) using a scanning electron microscope (SEM). Concentrations of REE, Y, and P were measured in order to test the different mechanisms for Li substitution. Ca, Fe, U, and Th were analyzed as potential tracers of alteration. Zircons were analyzed for 23 trace elements (Li, P, Ca, Ti, V, Fe, Y, REE, Th, and U) using an IMS-1280 ion microprobe in the WiscSIMS Laboratory at the University of Wisconsin, Madison, with analytical procedures similar to those in Page et al. (2007) and Lancaster et al. (2009). A primary $^{16}O^-$ beam with a current of 4 nA and a 10-kV accelerating voltage was defocused to a ~25-μm-diameter spot. An energy offset of −40 eV, associated with an energy slit of 44 eV, was applied, so that most molecular interferences are significantly reduced. In previous studies, a mass-resolving power (MRP) of 5,000–8,000 was applied in order to resolve LREE oxide interferences on HREE atomic ions (Lancaster et al. 2009; Page et al. 2007). However, because the focal points for ions differ slightly according to mass, the $^{7}Li^+$ peak is not flat at MRP = 8,000 when the instrument is optimized for REE peaks. Therefore, we applied MRP = 3,000 to preserve flatness of the Li

peak, allowing good precision of Li measurements. Hydride interferences to trace element peaks were not significant as zircon grains studied were anhydrous and most hydride interferences are fully resolved at MRP = 3,000. Oxide interferences on REE are lower in mass typically by 0.02 amu, requiring >8,600 mass-resolving power for a full separation from REE peaks. However, they are not significant for zircons, which show low abundances of LREE. In contrast, the contributions of LREE oxides to middle and heavy REE are significant for standard NIST-610 glass that contains all REE at the level of ~500 ppm. At MRP = 3,000 and energy offset of −40 eV, LREE oxide peaks appear on the low-mass shoulder of HREE peaks, which are easily identified in NIST-610. To solve this problem, the mass calibration of HREE peaks is adjusted slightly to measure the higher mass side of each spectrum that shows a flat top. Secondary ions were counted using a single ETP electron multiplier detector (EM) in the axial position using magnetic peak switching. Seven cycles of measurements were taken during an analysis. Only the last 5 cycles were integrated, and the first two cycles were used to stabilize the magnet. The counting and waiting times for analyzed isotopes are reported in supplementary information SI-1. The total analysis time per spot was 23 min, including 100 s of pre-sputtering.

During the analysis session, we used NIST-610 glass as a running standard, for which concentrations of REE are high (~500 ppm) and well characterized in the literature (Pearce et al. 1997), so that the standard provides minimum relative biases among REE concentrations and reliable REE patterns. The zircon standards 91500 (Cavosie et al. 2006; Wiedenbeck et al. 2004) and Xinjiang (Ushikubo et al. 2008) with known trace element concentrations were used to evaluate the matrix effects on relative sensitivity factor (RSF) between zircon and NIST-610 (Page et al. 2007; Ushikubo et al. 2008, see also supplementary information SI-2). We could not apply the matrix correction for P, Ca, V, and Fe as their concentrations in zircon standards are not known. The matrix effect is relatively limited for other elements, with an average factor of 1.2 between values determined using NIST-610 or Xinjiang zircon standards. Thus, the matrix effect on P, Ca, V, and Fe may be limited also. We estimated these concentrations using an averaged matrix correction between zircon and NIST-610 from other elements. The RSF for each element, estimated from the analyses of the above standards, is defined by the following equation:

$$\mathrm{RSF} = [\text{Element concentration}]_{\text{standard}} / [\mathrm{SiO_2}]_{\text{standard}} / [\text{isotope}^+ / {}^{30}\mathrm{Si}^+]_{\text{measured}}$$

RSFs are reported in supplementary information SI-2. The reproducibility of RSF for individual elements from NIST-610 glass was generally better than ±4% (2SE), due to high trace element concentrations. However, the reproducibility of trace elements in the 91,500 zircon standard is inversely correlated with concentration and varies from 10 to 42% (up to ±92% 2SE for Pr at 0.01 ppm; supplementary information SI-3).

For all data, each of the 5 cycles was checked for spikes (3SD) and none were found, suggesting that no analyses hit REE-rich inclusions such as a phosphate mineral. After analysis, each pit was imaged by SEM. No analyses have unusual pits (e.g., no porous pits or unusual shapes compared with other pits from the same session). Pits hitting cracks ($n = 16$) are not deemed accurate and have not been included in averages, as they tend to have higher LREE, Li, and Fe contents. Data from pits overlapping cracks are reported in Supplementary information SI-4.

Li isotope ratios

We measured Li isotope ratios of TTG and sanukitoid zircons by IMS-1280, using an axial electron multiplier (EM) instead of multiple EMs. We measured $^6Li^+$ (counting time = 10 s/cycle), $^7Li^+$ (1 s/cycle), and $^{28}Si^{2+}$ (2 s/cycle) by a magnet peak-switching analysis with 40 cycles. The $^{28}Si^{2+}$ peak was used to monitor the stability of the analysis. Other analysis conditions are similar to those used by Ushikubo et al. (2008). To summarize the analytical technique, the primary O^- beam was 10–15 μm diameter at the surface of the sample in Köhler illumination mode with ion current of 0.5–3 nA, depending on the Li content. NIST-612 glass ([Li] = 41.5 ± 2.9 ppm, δ^7Li = 31.2‰ ± 0.3‰; Kasemann et al. 2005; Pearce et al. 1996) was used as a running standard to evaluate instrumental stability. Average-measured values of 20 grains of Xinjiang zircon ([Li] = 6.4 ± 1.9 ppm, δ^7Li = 7.9 ± 2.1‰ (2SD); Ushikubo et al. 2008) were used to calibrate [Li] and δ^7Li of unknown samples. Values of δ^7Li are reported in standard per mil notation relative to the international Li standard, NIST SRM-8545 (LSVEC).

The δ^7Li values of Jack Hills zircons are from Ushikubo et al. (2008). We performed most (21) trace element analyses on visible pre-existing δ^7Li pits without repolishing.

Results

Trace elements

Type-1 domains

TTG and sanukitoid zircons from Superior Province, Canada The TTG and sanukitoid zircon data are reported in Tables 2 and 3, and chondrite-normalized patterns

(McDonough and Sun 1995) of Type-1 TTG and sanukitoid zircons are presented in Fig. 1a–b. Trace elements in sanukitoid zircons display a more restricted range and their abundance (143–335 ppm, average = 220 ± 59 ppm) is lower than in TTG zircons (165–804 ppm; average: 358 ± 159 ppm). Positive Ce and negative Eu anomalies are more pronounced in Type-1 TTG zircons, characterized by Ce/Ce* [$Ce/(La_N \times Pr_N)^{1/2}$] = 45–418 and Eu/Eu* [$Eu/(Sm_N \times Gd_N)^{1/2}$] = 0.3–1.0, whereas sanukitoid Type-1 zircons have Ce/Ce* = 24–311 and Eu/Eu* = 0.2–0.95.

The highest contents measured in these zircons are for Y, with 223–1,329 ppm in TTG zircons, and from 278 to 731 ppm in sanukitoid zircons, a narrower and slightly lower range compared with TTG. Phosphorus is also an important constituent in the analyzed zircons, reaching several hundred ppm. The range of [P] in Type-1 domains is similar: 79–291 ppm for TTG and 72–256 ppm for sanukitoid.

TTG zircons have 1.5–27.9 ppm Ti for TTG (average of 13.5 ± 17.2 ppm (2SD)), suggesting apparent temperatures between ~590 and 850°C, assuming equilibration, no pressure correction, $a(SiO_2) = 1$ and $a(TiO_2) = 0.7$ (Ferry and Watson 2007). Sanukitoid zircons have higher [Ti] than TTG, with 8.0–33.6 ppm [Ti] (average: 17.2 ± 13.3 ppm (2SD)), suggesting a range of apparent temperatures from ~720 to 865°C.

Ca content, which can be used as a tracer of alteration, is similar for TTG and sanukitoid zircons, with ranges from 0.1 to 4.8 ppm (one outlier at 443 ppm Ca) for TTG and 0.1–3.9 ppm for sanukitoid. Th and U contents range from 16 to 203 ppm and 33 to 340 ppm, respectively, in TTG Type-1 domains. These elements vary from 57 to 307 ppm and from 55 to 403 ppm, respectively, for Th and U, in sanukitoid Type-1 domains. Th/U ratios in sanukitoid zircons vary from 0.5 to 2.3, twice higher than in TTG zircons (0.2–1.2).

Lithium content reaches several tens of ppm in Type-1 zircon domains from both rock types. Lithium content is lower in TTG zircons (0.5–36 ppm) compared with sanukitoid zircons (2.2–79 ppm). For TTG and sanukitoid zircons, the atomic ratio (REE + Y)/(Li + P), representative of the Li-coupled substitution, ranges from 0.6 to 2.6 and from 0.4 to 1.6, respectively.

Jack Hills The Jack Hills data for twenty-five > 3.9-Ga and three 3.3- to 3.7-Ga detrital zircons are reported in Table 4, and normalized REE patterns of the Type-1 domains are presented in Fig. 1c. The total abundance of REE varies widely from 189 to 1,180 ppm (average = 594 ± 425 ppm), in agreement with previously published values determined by either ion microprobe or laser ablation mass spectrometry (Cavosie et al. 2006; Crowley et al. 2005; Hoskin 2005; Maas et al. 1992; Peck et al. 2001; Wilde et al. 2001; Trail et al. 2007). This range encompasses that of TTG and sanukitoid zircons and is in the range of crustal igneous zircons (Grimes et al. 2007, 2011; Hoskin and Schaltegger 2003). Ce and Eu anomalies are less pronounced than in TTG and sanukitoid zircons, with Ce/Ce* = 6.4–174 and Eu/Eu* = 0.1–1.0. For these Type-1 zircon domains, [Li] = 1.9–56 ppm, [P] = 46–682 ppm, [Ca] = 0.1–11 ppm, [Y] = 857–3,027 ppm. $(REE + Y)/(Li + P)_{at}$ ranges from 0.3 to 3.0. Th and U contents range from 6.7 to 260 ppm and from 20 to 273, respectively, and Th/U = 0.1–0.9. The values of [Ti] (2.8–14.1 ppm; average = 7.1 ± 5.4 (2SD)) in Jack Hills zircons are consistent with previous studies of Fu et al. (2008), Trail et al. (2007), and Harrison and Schmitt (2007), who reported [Ti] averages from 5.9 ± 6.6 ppm to 15.3 ± 15.1 ppm (2SD) for 91 Jack Hills zircons. This range of Ti values suggested apparent temperatures < 780°C. Values of [Ti] in Jack Hills zircons are in the range of, but have a lower average than TTG and sanukitoid zircons.

Type-2 domains

Six analysis pits on TTG, two on sanukitoid and five on Jack Hills zircons, display Type-2 REE patterns (Fig. 1d; Tables 2, 3, 4), with $La_N > 1$, $Pr_N > 10$, and $Sm_N/La_N < 50$ (e.g., Cavosie et al. 2006). These analyses represent 29, 9, and 18% of the total analysis pits in TTG, sanukitoid, and Jack Hills zircons, respectively. Type-2 compositions were measured in both the cores and the rims of zircons. Four of the Type-2 REE analyses (3 TTG and 1 Jack Hills) are on cores of zircons that display Type-1 REE compositions for the rim.

Type-2 analysis pits, as those from Type-1, have been carefully evaluated by SEM to determine whether re-crystallized zircon (disturbance in the CL pattern) or another phase is present, and each analysis cycle (5/analysis) has been examined to verify the absence of spikes (>3 SD) during an analysis. No spike in the cycle of any analysis was identified. CL imaging shows concentric or sector growth zoning, which argues against re-crystallization as a process to generate Type-2 domains (Supplementary information SI-5). Although no in situ geochronology is available for the specific sanukitoid and TTG zircons we analyzed, all Jack Hills analysis pits were made in zircon domains that were previously dated (Cavosie et al. 2004) with better than 85% concordance of U–Pb ages.

The total REE for the TTG and Jack Hills Type-2 analyses are higher than those from Type-1 patterns with averages of 563 and 1,395 ppm for Type-2, respectively, whereas total REE are similar for Type-1 and Type-2 analyses in sanukitoids. Due to LREE enrichment, Ce and

Table 2 Trace element in TTG zircons

Location	Type 1 zircons												
	C88-29-0 M								C92-30		DD81-32		
	5-4.2 Rim	6-3.2 Rim	7-2.1 Rim	7-6.1 Core	7-6.2 Rim	2-4.1 Core	7-7.3 Core	7-8.2 Rim	1-2.2 Rim	2-1.2 Rim	5-1.2 Rim	6-8.1 Core	6-8.2 Rim
Li	15.0	16.6	21.8	1.4	14.4	17.0	16.2	20.3	7.6	5.1	9.3	0.5	8.8
P	199	207	254	207	192	291	267	198	83	81	288	257	263
Ca	0.2	0.1	0.1	0.1	0.2	3.3	0.2	4.8	0.2	0.5	0.1	0.1	0.1
Ti	19.2	18.9	27.9	8.2	17.2	22.0	26.9	8.2	3.8	3.9	12.5	16.2	12.6
V	0.68	0.49	0.72	1.31	0.44	0.45	0.87	0.42	0.09	0.08	0.12	0.33	0.23
Fe	5.1	6.8	4.9	2.4	4.4	7.2	2.7	10.9	1.7	2.5	0.7	1.3	1.5
Y	438	387	412	822	349	589	461	451	346	263	547	1,329	503
La	0.03	0.02	0.01	0.02	0.02	0.04	0.02	0.06	0.01	0.00	0.01	0.01	0.00
Ce	33.7	31.5	33.6	38.6	27.1	33.2	30.6	41.1	19.5	22.4	6.7	10.1	6.6
Pr	0.2	0.2	0.3	0.6	0.2	0.8	0.3	0.2	0.0	0.1	0.1	0.2	0.0
Nd	2.1	1.6	3.1	7.3	2.7	7.3	3.1	1.6	0.9	0.8	1.0	2.2	0.8
Sm	3.1	3.1	4.3	12.0	2.9	7.5	4.7	3.0	1.2	1.2	1.6	5.9	1.6
Eu	0.9	0.7	1.0	2.3	0.5	1.5	1.2	0.8	0.5	0.3	0.3	0.7	0.2
Gd	5.1	4.1	5.0	11.9	3.8	7.8	6.4	4.7	3.1	2.7	4.3	13.3	4.3
Tb	6.1	5.3	6.6	15.4	5.1	9.9	8.3	6.0	3.3	3.3	4.9	15.8	4.4
Dy	39.8	35.0	40.5	85.8	32.5	57.7	46.7	38.4	25.8	22.4	48.8	130	43.2
Ho	12.8	10.6	11.7	23.7	10.3	16.9	13.9	11.9	8.8	8.1	17.9	41.6	15.0
Er	55.0	51.6	52.4	98.7	42.8	73.0	61.2	58.9	47.8	36.3	79.4	181	72.5
Tm	11.3	10.6	10.3	19.1	9.2	14.2	12.0	12.3	11.0	9.6	19.5	39.1	18.4
Yb	107	99.6	91.7	165	90.0	121	103	118	119	89.4	164	293	135
Lu	20.7	18.8	17.5	30.1	17.3	21.4	19.9	23.5	25.6	26.4	41.6	71.4	36.0
Th	129	103	144	203	76	150	115	157	40	63	18	46	16
U	159	164	160	173	117	147	126	224	78	100	33	54	34
δ^7Li (‰)	2.3 ± 2.2	4.1 ± 2.9	3.0 ± 1.9	−0.2 ± 7.4	4.2 ± 2.4	8.0 ± 2.4	2.7 ± 2.2	0.0 ± 2.2	0.7 ± 2.8	−2.7 ± 2.8	1.0 ± 4.0	−12.3 ± 9.9	2.0 ± 2.7
Th/U	0.81	0.63	0.90	1.17	0.65	1.02	0.91	0.70	0.51	0.63	0.55	0.86	0.48
(Y + REE)/(P + Li)	0.86	0.73	0.61	2.09	0.72	0.83	0.72	0.82	1.59	1.42	0.89	2.68	0.87
(Y + REE)/P	1.19	1.02	0.87	2.09	0.99	1.07	0.93	1.25	2.32	1.86	1.03	2.68	1.02
Σ REE (ppm)	298	273	278	510	244	373	311	320	266	223	390	805	338
Ca + Fe (ppm)	5.3	6.9	5.0	2.6	4.6	10.5	2.9	15.7	2.0	3.0	0.8	1.4	1.6
Ce/Ce*	101.9	116.0	137.8	84.0	108.9	48.5	101.9	82.4	224.5	418.5	55.9	62.2	
Eu/Eu*	0.70	0.59	0.68	0.58	0.49	0.61	0.64	0.67	0.77	0.58	0.31	0.25	0.21
$(Sm/La)_N$	185	228	535	1,009	232	349	433	81	210	1,226	234	1,015	–

Table 2 continued

Location	Type 2 zircons							
	DD86-25a		C88-29-0 M	C92-30	DD86-25a			
	2-2.3 Rim	5-3.2 Rim	5-4.1 Core	2-1.1 Core	2-2.2 Rim	3-6.1 Core	3-6.3 Rim	5-7.2 Rim
Li	6.9	35.6	1.9	0.3	11.4	3.6	8.4	57.6
P	79	168	234	407	279	201	107	224
Ca	0.3	443.1	5.7	226.8	189.4	16.1	9.0	185.0
Ti	1.5	3.7	25.6	13.3	7.7	5.0	4.7	9.8
V	0.04	0.03	1.15	1.15	0.83	0.74	0.31	0.22
Fe	6.7	367	17.3	1.8	4.0	17.2	13.4	532
Y	223	765	855	896	555	1,223	342	1,076
La	0.02	0.01	0.67	0.74	0.95	4.70	2.50	4.26
Ce	3.3	12.5	43.5	33.2	11.2	24.3	12.6	44.3
Pr	0.0	0.0	2.1	1.1	1.3	5.0	3.1	7.8
Nd	0.2	1.1	15.9	10.8	5.4	29.9	14.7	46.6
Sm	0.5	2.2	16.7	12.7	3.7	16.0	6.2	14.8
Eu	0.1	0.3	3.7	1.9	0.7	2.2	0.3	1.9
Tb	1.5	5.5	13.5	12.0	5.3	14.9	2.1	9.3
Gd	1.8	6.5	18.5	18.2	6.7	19.2	3.3	12.0
Dy	16.2	60.3	95.5	101	48.4	126	24.2	90.9
Ho	5.7	21.8	26.1	29.0	17.1	36.6	7.9	28.7
Er	30.7	103	105	115	77.0	158	42.2	139
Tm	8.3	24.8	20.2	26.2	18.2	35.7	10.7	30.8
Yb	75.1	214	170	203	150	264	89.3	219
Lu	21.4	58.4	32.0	47.3	38.8	66.1	27.5	58.0
Th	30	142	220	93	55	168	57	268
U	164	340	188	67	117	245	194	397
δ^7Li (‰)	0.6 ± 3.0	12.5 ± 2.3	−3.5 ± 5.3	−5.8 ± 17.7	−1.7 ± 2.4	−24 ± 9.6	−8.1 ± 3.4	−6.9 ± 3.4
Th/U	0.18	0.42	1.17	1.40	0.46	0.68	0.29	0.68
(Y + REE)/(P + Li)	1.07	1.18	1.88	1.19	0.89	2.98	1.26	1.12
(Y + REE)/P	1.54	2.43	1.96	1.19	1.08	3.25	1.75	2.57
Σ REE (ppm)	165	510	563	612	385	803	246	708
Ca + Fe (ppm)	7.0	810	22.9	229	193	33.3	22.4	717
Ce/Ce*	45.5	149.5	8.7	8.6	2.4	1.2	1.1	1.8
Eu/Eu*	0.28	0.29	0.75	0.47	0.46	0.44	0.23	0.50
$(Sm/La)_N$	55	321	42	29	7	6	4	6

Sample name are as follow: $x - x{\cdot}y : x - x$ zircon number; y: spot number in the zircon

SiO_2 content of whole rocks, when measured: C92-30: SiO_2 = 64.9 wt%; DD86-25a: SiO_2 = 68.9 wt% (King et al. 1998)

Table 3 Trace element in sanukitoid zircons

Location	Type 1 zircons								
	C92-31				DD96-4				
	2-6.2 Rim	7-1.1 Core	7-10.1 Core	11-8.3 Rim	3-6.1 Rim	5-8.1 Core	5-11.2 Core	6-5.1 Rim	11-1.1 Rim
Li	2.3	3.7	2.2	5.2	38.3	41.3	22.4	16.5	32.2
P	149	206	142	187	152	257	233	161	195
Ca	0.2	0.2	0.2	0.2	1.0	0.1	0.2	0.2	0.3
Ti	12.9	10.6	12.4	17.5	8.0	8.9	14.6	15.7	10.9
V	0.38	0.29	0.48	0.67	0.22	0.21	0.37	0.56	0.40
Fe	1.4	1.5	2.7	2.7	2.4	1.5	1.3	1.3	1.5
Y	408	544	486	516	347	526	411	290	385
La	0.01	0.01	0.02	0.04	0.01	0.02	0.01	0.02	0.02
Ce	55.8	74.5	91.5	85.9	31.5	44.6	33.4	30.2	47.7
Pr	0.2	0.3	0.3	0.5	0.1	0.3	0.3	0.1	0.2
Nd	2.6	2.4	3.6	5.8	1.3	2.5	2.4	1.5	1.7
Sm	4.2	4.5	5.1	6.3	2.1	3.7	3.5	2.7	3.2
Eu	1.2	1.2	1.3	2.0	0.4	0.7	0.7	0.4	0.6
Gd	4.4	4.8	4.3	6.3	2.4	4.6	3.8	2.3	3.2
Tb	4.4	4.8	4.3	6.3	2.4	4.6	3.8	2.3	3.2
Dy	30.5	35.5	30.1	44.8	23.2	34.3	29.0	20.5	24.4
Ho	8.3	9.7	8.1	11.5	6.6	10.3	7.7	5.4	6.6
Er	33.2	39.7	31.8	44.1	30.9	45.3	33.2	22.6	28.0
Tm	9.2	11.1	9.0	12.0	8.8	13.3	10.2	6.8	8.5
Yb	60.0	62.3	48.8	85.6	72.2	97.7	68.8	45.5	53.4
Lu	16.4	17.0	14.6	21.2	20.3	29.0	20.4	13.9	16.1
Th	69.8	109	150	169	115	160	78	57.3	131
U	54.6	99.2	119	104	218	243	105	73.2	159
δ^7Li (‰)	-2.1 ± 4.0	5.3 ± 4.6	7.1 ± 5.2	1.0 ± 2.7	0.5 ± 3.2	8.9 ± 3.6	11.9 ± 3.7	1.0 ± 3.2	6.8 ± 3.2
Th/U	1.28	1.10	1.26	1.62	0.53	0.66	0.75	0.78	0.82
(Y + REE)/(P + Li)	1.31	1.22	1.61	1.30	0.52	0.58	0.60	0.61	0.55
(Y + REE)/P	1.42	1.32	1.74	1.48	1.18	1.05	0.90	0.92	1.00
Σ REE	232	269	254	335	203	291	218	155	198
Ca + Fe (ppm)	1.6	1.6	2.9	3.0	3.4	1.6	1.5	1.5	1.9
Ce/Ce*	265.7	311.1	290.2	152.3	205.6	132.8	137.7	132.7	193.3
Eu/Eu*	0.82	0.80	0.84	0.95	0.50	0.49	0.58	0.53	0.55
$(Sm/La)_N$	552	598	433	284	337	282	450	228	308

Location	DD96-8					DD96-10			
	1-8.1 Core	3-8.1 Core	4-8.1 Core	7-9.1 Core	7-9.2 Rim	1-6.1 Core	2-4.1 Rim	3-8.1 Rim	4-8.3 Rim
Li	79.0	45.9	44.2	30.0	32.8	14.1	32.0	17.3	16.2
P	227	168	237	164	132	211	149	165	72
Ca	0.2	0.7	0.2	0.2	1.7	0.5	1.1	1.3	3.9
Ti	19.4	18.5	33.6	20.7	20.4	27.2	13.0	22.8	21.7
V	0.22	0.23	0.27	0.43	0.30	0.57	0.20	0.43	0.47
Fe	5.4	3.3	2.4	5.4	10.2	0.7	8.3	0.9	1.6
Y	494	367	411	628	335	731	278	327	338
La	0.01	0.01	0.02	0.02	0.02	0.09	0.01	0.02	0.03
Ce	23.0	16.3	15.5	14.4	12.5	41.8	41.3	30.8	39.3

Table 3 continued

Location	DD96-8					DD96-10			
	1-8.1 Core	3-8.1 Core	4-8.1 Core	7-9.1 Core	7-9.2 Rim	1-6.1 Core	2-4.1 Rim	3-8.1 Rim	4-8.3 Rim
Pr	0.3	0.1	0.3	0.3	0.1	1.9	0.2	0.4	0.3
Nd	3.6	1.3	3.5	2.1	1.6	16.7	1.6	3.3	1.8
Sm	4.3	2.3	4.4	4.0	2.0	17.0	2.5	4.2	3.0
Eu	0.4	0.2	0.4	0.4	0.2	2.5	0.3	0.6	0.7
Tb	4.3	2.5	3.7	4.9	2.3	8.9	2.1	3.6	2.7
Tb	4.3	2.5	3.7	4.9	2.3	8.9	2.1	3.6	2.7
Dy	34.2	22.7	28.7	40.6	20.1	59.3	15.7	23.5	20.4
Ho	9.1	6.6	7.5	10.8	5.8	13.0	4.0	6.3	5.9
Er	37.4	26.9	30.0	44.8	23.1	49.2	18.1	23.8	24.8
Tm	10.8	8.9	9.0	13.2	8.2	13.2	5.7	6.6	7.7
Yb	69.1	57.9	52.4	81.2	50.4	73.7	38.2	45.1	53.7
Lu	19.4	16.6	15.5	22.4	14.4	22.0	10.3	11.8	13.5
Th	307	148	150	196	122	181	117	75.1	215
U	403	248	194	246	182	138	151	77.8	91.3
δ^7Li (‰)	7.5 ± 3.2	4.4 ± 3.4	3.7 ± 3.7	9.8 ± 3.4	2.0 ± 3.4	7.0 ± 3.7	6.1 ± 3.2	8.5 ± 3.2	13.2 ± 3.6
Th/U	0.76	0.60	0.77	0.80	0.67	1.31	0.77	0.97	2.35
(Y + REE)/(P + Li)	0.39	0.45	0.43	0.95	0.55	1.28	0.46	0.65	1.12
(Y + REE)/P	1.06	1.07	0.84	1.81	1.23	1.70	0.94	1.00	2.38
Σ REE	222	166	176	245	144	332	143	165	177
Ca + Fe	5.6	4.0	2.6	5.6	11.9	1.3	9.5	2.2	5.5
Ce/Ce*	87.9	102.5	52.5	52.7	72.5	24.2	266.6	80.5	107.5
Eu/Eu*	0.26	0.23	0.27	0.30	0.27	0.62	0.35	0.49	0.76
$(Sm/La)_N$	513	389	429	391	217	325	612	299	197

Location	Type 2 zircons			
	7-9.1 Core	7-9.2 Rim	DD96-4 5-9.1 Core	DD96-8 5-10.1 Core
Li	20.4	18.0	19.9	49.6
P	156	211	184	183
Ca	2.3	1.7	0.4	9.1
Ti	23.9	10.4	11.3	29.0
V	0.44	0.26	0.92	0.93
Fe	2.0	6.2	3.7	3,085
Y	402	363	477	313
La	0.02	0.04	0.31	2.44
Ce	41.1	40.0	46.0	20.5
Pr	0.3	0.2	0.6	1.8
Nd	4.2	1.8	2.8	7.6
Sm	5.4	3.3	4.1	4.7
Eu	0.7	0.4	0.7	0.3
Tb	4.1	2.9	4.3	2.6
Tb	4.1	2.9	4.3	2.6
Dy	29.6	22.5	35.1	19.6
Ho	7.1	6.0	9.8	5.3
Er	29.1	26.3	36.4	23.8
Tm	7.7	8.1	11.8	7.1

Table 3 continued

Location	Type 2 zircons			
			DD96-4	DD96-8
	7-9.1 Core	7-9.2 Rim	5-9.1 Core	5-10.1 Core
Yb	47.6	53.1	72.2	43.3
Lu	13.6	14.8	21.2	13.6
Th	108	124	132	141
U	92.6	78.0	131	213
δ^7Li (‰)	9.7 ± 3.4	14.2 ± 3.4	3.1 ± 3.2	5.9 ± 3.2
Th/U	1.17	1.60	1.01	0.66
(Y + REE)/(P + Li)	0.74	0.64	0.70	0.32
(Y + REE)/P	1.17	0.95	1.31	0.85
Σ REE	196	183	252	156
Ca + Fe	4.3	7.9	4.1	3,093.9
Ce/Ce*	116.3	103.1	25.3	2.4
Eu/Eu*	0.45	0.37	0.49	0.28
$(Sm/La)_N$	405	144	22	3

Sample name are as follows: $x - x$·y: $x - x$ zircon number; y: spot number in the zircon

SiO2 content of whole rocks, when measured: C92-31: $SiO_2 = 58.95$ wt%; DD96-4: $SiO_2 = 62.7$ wt%; DD96-10: $SiO_2 = 57.2$ wt% (King et al. 1998)

Eu anomalies are less pronounced in Type-2 patterns than in Type-1: Ce/Ce* is lower than 9, 25, and 13 and Eu/Eu* does not exceed 0.7, 0.5, and 0.5 for TTG, sanukitoid, and Jack Hills zircons, respectively.

Type-1 and Type-2 zircon domains from TTG, sanukitoid, and Jack Hills are reported in two plots (Fig. 2a–b) where unaltered magmatic versus non-magmatic compositions can be distinguished. In Fig. 2a, representing normalized Sm/La ratios plotted against [La], Type-1 domains of TTG, sanukitoid, and Jack Hills zircons have high $(Sm/La)_N$ (>10) associated with low [La] (<0.1 ppm), representative of unaltered magmatic zircons (Grimes et al. 2009; Hoskin 2005). Type-2 REE patterns are marked by flatter LREE profiles (Fig. 1), leading to Sm/La-normalized ratios lower than for Type-1 REE patterns. Type-2 REE patterns have lower $(Sm/La)_N$ (3–39; slightly overlapping with the lower range for Type-1 REE) associated with higher [La] (0.3–4.7 ppm) than Type-1 REE patterns. Type-2 zircons in this study have lower [La] but higher $(Sm/La)_N$ than hydrothermal zircons (Hoskin 2005), but have compositions matching those of porous zircons (Grimes et al. 2009), although no porous texture has been observed in our zircons.

Li and P contents in Type-2 zircon domains are mostly similar to Type-1 zircons for TTG and sanukitoid (see Tables 2, 3, and 4), whereas these two elements tend to be enriched in Jack Hills zircon domains with Type-2 REE patterns, with average compositions of 31 and 48 ppm Li and 260 and 1,150 ppm P for Type-1 and Type-2 zircon domains, respectively. Similarly, Th/U ratios are similar in Type-2 and Type-1 zircon domains from TTG (from 0.3 to 1.4, only two analyses are >1) and from sanukitoid (0.7–1.0), whereas Jack Hills Type-2 zircon domains have higher Th/U (0.6–4.4) than Type-1 (Th/U = 0.1–0.9). Type-2 domains from the three rocks types have Th and U contents 8–10 and 2–3 times higher (54.5–3,108 ppm Th and 66.5–698 ppm U) than in Type-1 (6.74–307 ppm Th and 19.7–403 ppm U), suggesting that Type-2 domains have suffered more radiation damage, due to the α-decay of U and Th (Murakami et al. 1991).

Alteration in zircons has also been investigated using [Ca] and [U] (Fig. 2b). Ca content ranges are slightly higher in all Type-2 zircon analyses compared with Type-1, with 22–717 ppm in TTG, 4–3,093 ppm in sanukitoid, and 94–2,796 ppm in Jack Hills. While the amount of radiation damage is influenced by several factors including composition, age, and thermal history, simple correlations with [U] are often found. Rayner et al. (2005) reported compositions of altered Archean zircons, which have [U] > 2,000 ppm and [Ca] > 50 ppm (Fig. 2b). High [U] in Archean zircon could represent either metamict or re-crystallized areas. The patchy appearance of the altered zircons in Rayner et al. (2005) is interpreted to reflect fluid alteration. The authors do not report evidence of re-crystallization. The low [Ca] (<15 ppm) and [U] (<400 ppm) of Type-1 domains from the present study attest to their unaltered magmatic values. The fields of fluid-altered zircons, with [U] > 2,600 ppm and [Ca] > 200 ppm and porous zircons (Grimes et al. 2009), with compositions

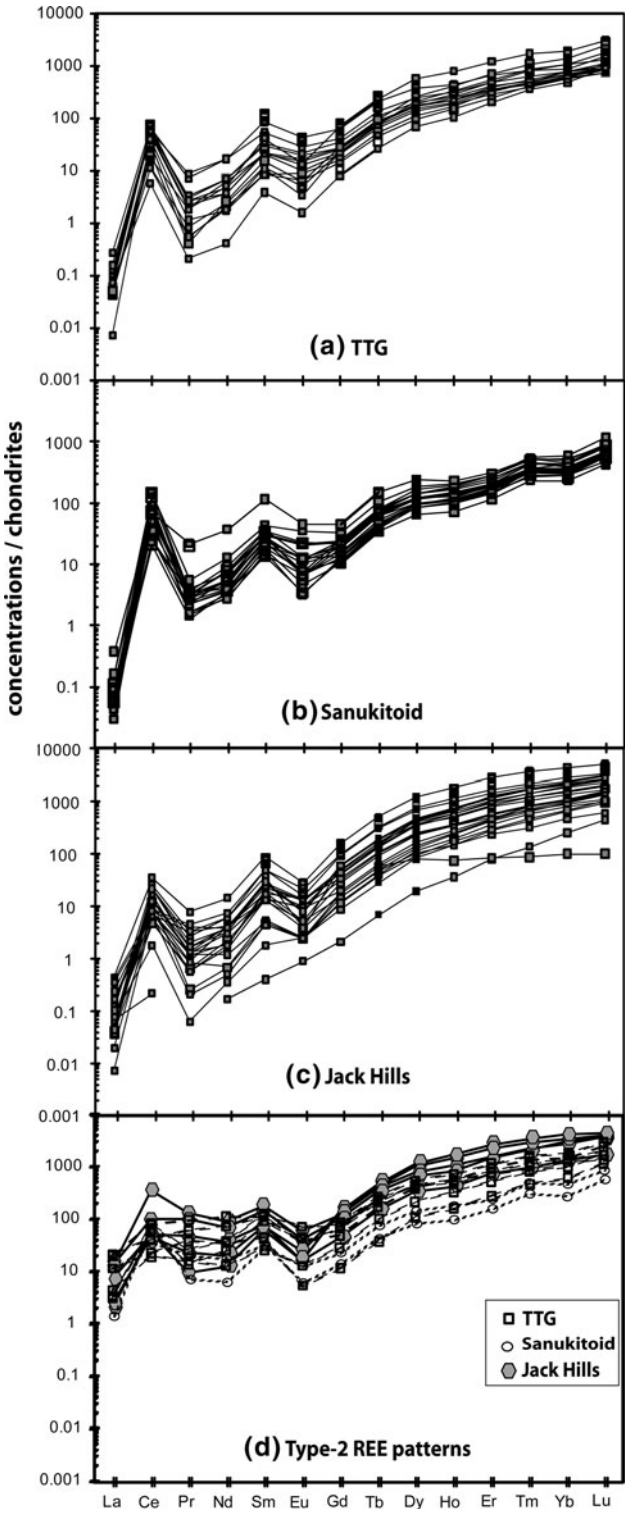

Fig. 1 Chondrite-normalized patterns of rare earth elements (REE) in Archean (4.35- to 2.6-Ga) Type-1 igneous zircons from tonalites, trondhjemites, and granodiorites (TTG) (**a**), sanukitoids (**b**), Jack Hills > 3.9-Ga detrital suite (**c**), and Type-2 REE patterns (**d**)

between unaltered and altered zircons, are also plotted. The Type-2 domains of this study are significantly higher in [Ca] than the Type-1 domains (Fig. 2b; Tables 2, 3, 4). They have similar [Ca] but lower [U] than porous zircons (Grimes et al. 2009) and plot outside the field for altered zircons. Seven Type-2 domains are in the unaltered zircon field, whereas the six other Type-2 domains plot at higher [Ca] between altered and unaltered fields.

Li isotope ratios

Li isotope ratios of TTG and Sanukitoid zircons are plotted against Li content in Fig. 3 for both Type-1 and Type-2 domains. For comparison, those of Jack Hills zircons are shown in Fig. 3 using newly obtained REE abundance data. No systematic relation between Li content and/or δ^7Li could be seen between Type-1 and Type-2 domains for the three rock types. TTG zircons have δ^7Li from −12 to +8‰ for the Type-1 domains and from −24 to −2‰ for Type-2 domains. The two extremely negative values (−24, −12‰) are associated with high internal error (±10‰, 2SD) due to low Li contents (3.6 and 0.5 ppm, respectively). The sanukitoid Type-1 and Type-2 domains display narrower ranges and higher Li isotope ratios than TTG (−2 to +14‰ for Type-1 domains and +3 to +6‰ for the Type-2 domains). Li isotope ratios for the Jack Hills zircons vary from −18 to +12‰ for Type-1 and from −16 to +2‰ for Type-2 domains. The values of δ^7Li for 60% of the Jack Hills zircons match those of TTGs and sanukitoids; however, 40% of the >3.9-Ga zircons have lower values of δ^7Li between −5 and −19‰ that are not seen in the Archean granitoid suite. For the three samples, there is no correlation between Li content and Li isotopic composition other than the larger uncertainties in δ^7Li for low [Li] grains.

The significance of chemical diffusion of Li can be tested by examining core versus rim zoning of [Li]. Two analyses (core and rim) have been performed in 6 pairs of Type-1 domains (2 TTG, 2 sanukitoid, and 2 Jack Hills; Fig. 4). The TTG and Jack Hills zircons display cores with [Li] significantly different from rims, showing that neither [Li] nor δ^7Li has become homogenized. There is no consistent relationship among these zircons, some cores are lower in [Li], while others are the same as the rim, and one core is richer in Li.

Discussion

The comparison of our data with unaltered magmatic zircons suggests that Type-1 domains are representative of unaltered, typical magmatic zircons, whereas Type-2 domains of this study do not preserve magmatic compositions and represent areas with radiation damage. The intermediate compositions of the Type-2 domains between magmatic and hydrothermal (Fig. 2a–b) are consistent with the interpretation that these are altered zones within a zircon that were

Table 4 Trace element in Jack Hills zircons

Location	Type 1 zircons								
	JH-13b 2.5NM		JH-13b 2.5 M						JH-13b 5 M
	19-1.5 Core	20-2.1 Core	2-1.1 Core	6-3.1 Rim	8-4.1 Rim	8-4.3 Core	13-2.1 Rim	24-1.1 Core	4-2.3 Core
Li	1.9	8.2	14.8	43.1	56.2	45.2	29.5	40.9	34.8
P	281	46	166	180	166	196	363	80	548
Ca	0.23	0.47	0.68	0.11	3.6	3.1	4.8	6.3	11.2
Ti	4.5	2.8	5.3	5.9	6.1	7.7	5.1	7.8	14.1
V	1.11	0.00	0.06	0.01	0.06	0.02	0.15	0.00	0.68
Fe	6.6	3.2	4.0	7.2	107.3	44.3	11.6	19.8	231.1
Y	1,651	79	605	605	418	454	941	156	3,141
La	0.01	0.02	0.02	0.01	0.04	0.06	0.02	0.01	0.11
Ce	13.6	0.1	3.1	10.5	3.6	4.6	8.2	2.9	21.6
Pr	0.2	0.0	0.1	0.1	0.1	0.1	0.1	0.1	0.7
Nd	2.8	0.1	0.7	0.9	0.3	0.6	1.5	1.1	6.7
Sm	7.5	0.1	2.0	2.4	0.8	0.8	4.2	2.0	13.1
Eu	0.9	0.1	0.6	0.3	0.1	0.1	0.8	0.2	1.6
Gd	18.9	0.4	6.2	5.6	3.0	3.6	9.9	3.5	31.8
Tb	20.2	0.3	7.3	6.5	2.7	3.3	11.4	3.6	34.0
Dy	172.1	4.8	59.4	55.8	32.3	34.8	89.3	20.3	302
Ho	56.0	2.1	19.5	20.1	13.5	14.1	28.8	4.2	103
Er	235	13.1	82.0	91.1	69.6	74.1	129	13.7	455
Tm	48.7	3.4	17.2	20.4	16.1	17.5	26.0	2.2	90.1
Yb	404	42.2	151	174	156	164	220	16.6	716
Lu	77.2	11.3	27.7	35.7	33.4	34.1	41.8	2.5	125
Th	73	7	19	82	27	39	63	11	260
U	78	20	41	199	193	163	108	156	273
δ^7Li (‰)[a]	-6.9 ± 6.9	-1.5 ± 3.7	-11.8 ± 3.3	1.4 ± 3.3	-18.4 ± 3.3	-10.5 ± 2.0	2.3 ± 3.3	-9.7 ± 2.2	-12.1 ± 2.8
δ^{18}O (‰)[a, b]	6 ± 0.3	8.2 ± 0.3	n.d.	6.6 ± 0.23	5.8 ± 0.23	6.0 ± 0.23	6.4 ± 0.32	7.5 ± 0.32	4.5 ± 0.32
Th/U	0.93	0.34	0.46	0.41	0.14	0.24	0.58	0.07	0.95
(Y + REE)/(P + Li)	3.00	0.54	1.32	0.83	0.52	0.60	0.96	0.27	2.26
(Y + REE)/P	3.10	1.03	1.91	1.82	1.40	1.29	1.35	0.96	2.98
Σ REE	1,057	78	376	423	331	352	571	73	1,900
Ca + Fe (ppm)	6.8	3.6	4.7	7.3	111	47.4	16.4	26.2	242.3
Ce/Ce*	54.3	0.0	24.5	72.5	16.3	13.9	40.0	30.1	18.8
Eu/Eu*	0.23	0.98	0.48	0.22	0.28	0.26	0.37	0.25	0.24
$(Sm/La)_N$	868	6	193	344	37	22	430	379	206
Ages[b]	4,066	3,875	4,125	4,089	4,007	4,007	4,081	4,299	3,904

Location				JH-54a 2.5NM			JH-54a 5 M		
	6-2.1 Rim	10-4.1 Core	22-1.1 Rim	17.1 Rim	34.1 Core	58.1 Core	77.1 Core	78.1 Core	78.2 Rim
Li	14.4	18.4	39.3	45.4	42.7	41.9	7.0	37.2	16.3
P	166	105	190	115	164	457	316	280	151
Ca	9.4	0.39	5.8	0.41	5.1	2.2	2.1	0.14	5.6
Ti	10.9	3.9	9.6	5.9	7.7	10.8	5.2	8.5	8.4
V	0.22	0.00	0.06	0.00	0.04	0.08	0.76	0.27	0.04
Fe	206.2	6.7	45.0	46.7	6.2	8.5	32.9	5.5	536
Y	1,337	290	1,190	381	556	1,079	1,896	978	280
La	0.10	0.02	0.03	0.01	0.04	0.02	0.04	0.00	0.08
Ce	4.9	1.1	6.5	7.5	4.7	16.0	5.4	4.8	4.3
Pr	0.4	0.0	0.1	0.0	0.1	0.3	0.4	0.1	0.3
Nd	1.8	0.2	0.9	0.3	1.4	2.9	3.5	0.8	1.9
Sm	3.4	0.3	3.1	0.7	2.1	5.6	7.4	2.8	1.9
Eu	0.7	0.1	0.6	0.1	0.5	0.2	1.3	0.3	0.3
Tb	10.3	1.8	9.4	2.5	4.0	11.7	19.7	8.2	2.9
Gd	10.7	2.0	10.2	2.3	4.4	13.0	22.6	9.5	3.6
Dy	111	20.6	106	28.5	42.2	99.9	186	88.2	25.3
Ho	40.1	8.7	37.5	11.1	15.8	32.6	64.8	30.1	8.4
Er	207	45.4	172	58.6	77.4	149	271	137	39.4
Tm	43.5	10.4	34.6	14.3	19.5	30.2	55.1	29.6	7.9
Yb	384	106	304	136	187	252	460	263	77.6
Lu	74.7	22.8	56.5	24.3	38.7	49.9	81.9	50.9	15.2

Table 4 continued

Location	JH-54a 2.5NM						JH-54a 5 M		
	6-2.1 Rim	10-4.1 Core	22-1.1 Rim	17.1 Rim	34.1 Core	58.1 Core	77.1 Core	78.1 Core	78.2 Rim
Th	53	11	86	80	63	144	69	88	38
U	111	43	136	231	163	157	86	181	107
δ^7Li (‰)	−0.3 ± 3.7	−4.7 ± 2.5	−15.9 ± 2.8	6.5 ± 3.1	11.8 ± 3.1	3.6 ± 1.9	−11.8 ± 3.4	4.5 ± 3.1	1.5 ± 3.1
δ^{18}O (‰)	5.4 ± 0.32	4.7 ± 0.3	6.2 ± 0.3	5.3 ± 0.6	6.5 ± 0.6	6.4 ± 0.6	6.4 ± 0.6	7.4 ± 0.6	6.2 ± 0.6
Th/U	0.48	0.26	0.64	0.34	0.39	0.92	0.80	0.49	0.36
(Y + REE)/(P + Li)	2.99	0.81	1.61	0.61	0.80	0.68	2.83	1.11	0.65
(Y + REE)/P	4.27	1.52	3.27	1.81	1.84	1.23	3.14	1.84	1.00
Σ REE	894	220	741	286	398	663	1,180	626	189
Ca + Fe	216	7.1	50.8	47.1	11.3	10.7	35.0	5.6	542
Ce/Ce*	6.4	25.6	24.7	118.1	16.4	44.9	10.0	73.2	6.4
Eu/Eu*	0.38	0.62	0.32	0.33	0.57	0.08	0.32	0.19	0.38
$(Sm/La)_N$	59	24	162	117	90	378	306	977	38
Ages[b]	4,229	3,631	4,113	4,178	4,165	4,063	4,282	4,046	3,362

Location	JH-54a 10 M		JH-13a 2.5NM			Type 2 zircons				
						JH-13b 5 M			JH-54a 10 M	
	81.2 Rim	90.2 Rim	3-6.1 Rim	3-4.1 Core	5-5.1 Core	14-1.1 Core	14-4.2 Core	22-2.1 Rim	90.1 Core	D7.1 Core
Li	30.1	30.8	35.6	35.9	44.0	50.2	76.4	49.3	24.9	39.1
P	267	157	249	652	682	1,066	766	2,893	669	350
Ca	0.14	0.21	1.2	1.5	1.7	81.6	143	464	29.7	3.9
Ti	8.7	3.0	8.9	7.1	5.0	31.8	28.3	109.8	26.5	35.0
V	0.12	0.01	0.33	0.04	0.02	4.02	2.11	12.57	0.71	0.09
Fe	5.0	19.8	5.7	12.1	12.4	531	441	2,332	1,188	89.8
Y	1,062	302	685	1,338	1,358	857	1,568	1,729	2,586	3,027
La	0.01	0.00	0.01	0.01	0.01	1.81	3.20	3.09	0.62	0.49
Ce	7.8	4.2	5.0	13.4	13.4	32.7	63.3	231.5	28.6	35.9
Pr	0.1	0.0	0.1	0.2	0.2	4.6	9.5	12.4	2.1	0.9
Nd	1.9	0.2	2.0	1.8	1.8	18.1	34.1	43.3	9.7	5.8
Sm	3.8	0.7	2.6	4.3	4.5	12.4	22.8	28.5	11.3	9.7
Eu	0.7	0.1	0.8	0.4	0.5	1.0	2.5	3.6	1.5	1.0
Tb	8.6	2.3	6.8	11.5	12.1	9.1	21.5	24.7	26.6	28.9
Gd	10.0	2.2	7.7	12.8	11.8	8.4	21.8	29.3	27.8	29.2
Dy	91.1	23.4	62.5	120	120	88.1	167	201	254	291
Ho	33.5	10.1	20.7	41.3	42.5	24.5	48.4	63.8	83.5	99.3
Er	161.6	47.2	96.3	190	193	125	240	258	370	445
Tm	35.6	11.7	20.5	41.2	41.4	24.8	54.5	57.3	74.7	85.9
Yb	322.5	114	185	347	355	224	530	481	594	697
Lu	64.9	25.8	37.3	63.7	67.2	43.6	97.3	94.6	100.6	110.7
Th	68	24	51	75	79	313	418	3,108	303	189
U	142	108	161	110	119	254	582	698	270	322
δ^7Li (‰)	8.1 ± 1.8	−0.6 ± 1.7	5.7 ± 2.2	5.4 ± 3.0	1.0 ± 3.0	−13.5 ± 2.8	−8.3 ± 2.5	−15.9 ± 2.5	0.7 ± 3.1	1.7 ± 3.1
δ^{18}O (‰)	7.2 ± 0.6	6.4 ± 0.6	6.6 ± 0.3	6.6 ± 0.43	6.4 ± 0.33	6.6 ± 0.3	5.8 ± 0.3	5.9 ± 0.3	6.3 ± 0.6	5.4 ± 0.6
Th/U	0.48	0.22	0.32	0.68	0.67	1.23	0.72	4.45	1.12	0.59
(Y + REE)/(P + Li)	1.37	0.54	0.85	0.85	0.79	0.62	0.46	0.32	1.70	2.89
(Y + REE)/P	2.14	1.08	1.46	1.08	1.05	0.84	0.61	0.35	2.02	4.50
Σ REE	742	242	447	847	864	617	1,316	1,532	1,584	1,841
Ca + Fe	5.1	20.0	6.9	13.6	14.1	613	584	2,796	1,218	93.7
Ce/Ce*	49.8	174.3	38.1	77.7	78.8	2.7	2.8	9.0	6.0	13.0
Eu/Eu*	0.38	0.34	0.58	0.19	0.19	0.28	0.34	0.41	0.26	0.18
$(Sm/La)_N$	554	634	350	788	696	11	12	15	31	33
Ages[b]	4,103	4,030	4,006	4,041	4,021	4,033	4,068	4,148	4,263	4,348

Sample name are as follows: x − x·y: x − x zircon number; y: spot number in the zircon

[a] Values from Ushikubo et al. (2008)

[b] Values from Cavosie et al. (2006)

[Li] values are from this study

n.d.: not determined

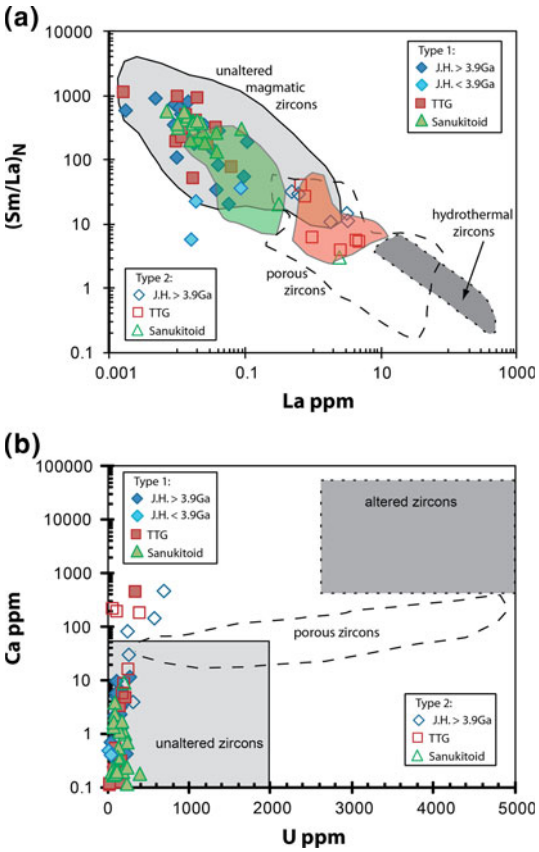

Fig. 2 **a** $(Sm/La)_N$ compared with La ppm (modified after Grimes et al. 2009; Hoskin 2005) and **b** Ca ppm versus U ppm (modified after Rayner et al. 2005). Type-1 domains (igneous) are represented by *filled symbols*, and Type-2 by *open symbols*. "J. H." (*diamonds*) is for Jack Hills. **a** Shows the field of unaltered magmatic zircons (*gray*; Grimes et al. 2009; Hoskin 2005), the field of porous zircons (*dashed line* delimited; Grimes et al. 2009), and the field of hydrothermal zircons, crystallized directly from aqueous fluids, defined by 13 analyses of visibly porous zircons from 4 rocks from the Boggy Plain pluton, SE Australia (*doted line* delimited *gray*; Hoskin 2005). Are also plotted the Type-1 (*green field*) and Type-2 (*pink field*) analyses for Jack Hills previously published by Cavosie et al. (2006). Type-1 domains are distinct from hydrothermal or altered zircons. Type-1 data plot in the magmatic field, whereas Type-2 zircons plot in the field of porous altered zircons

originally of igneous genesis rather than new zircon precipitated by hydrothermal processes. Accordingly, it is possible that U- and Th-rich domains of a zoned igneous zircon can become Type-2, while less radiogenic Type-1 domains of the same crystal preserve magmatic geochemistry. Thus, only data of Type-1 zircon domains are used for further discussion of igneous compositions.

Li-coupled substitutions and Li diffusion in zircons

Li is a significant trace element in zircon of this study (2–79 ppm by wt% in Type-1 domains, Fig. 3). The ratios of $[(Y + REE)/(Li + P)]_{atomic}$ calculated for TTG, sanukitoid, and Jack Hills Type-1 zircon analyses have an

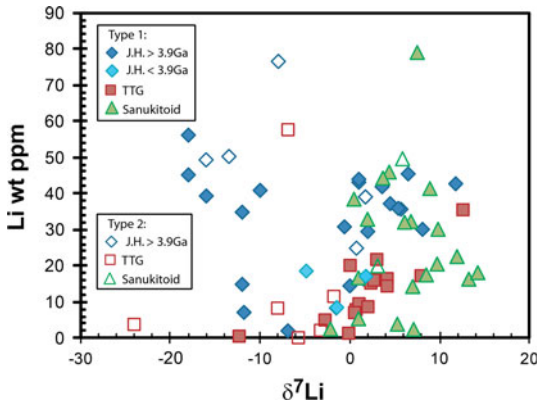

Fig. 3 [Li] versus δ^7Li of Type-1 and Type-2 zircon domains. Type-1 and Type-2 zircons are similar in [Li] and δ^7Li

average of 1.0 ± 0.7 (2SD) for all but six of 58 measurements in this study (Fig. 5). A similar range of values ($[(Y + REE)/(Li + P)]_{atomic} = 1.23 \pm 1.2$ (2SD); 10 analyses) is reported by Ushikubo et al. (2008) for Jack Hills zircons. Ninety percent of the present data plot around $[(Y + REE)/(Li + P)]_{atomic} = 1.0 \pm 0.7$ (2SD), implying that the Li and REE + P-coupled substitution (Eq. 2) is dominant in zircon (Ushikubo et al. 2008). Because of the predominance of the charge-balancing coupled substitution (Eq. 2), there is no a priori requirement that chemical diffusion of interstitial Li should be faster than ^{VIII}Li diffusion in zircons. Li chemical diffusion is dominantly linked to REE diffusion, which is slow in zircon (Cherniak et al. 1997; Cherniak and Watson 2003). Other substitutional mechanisms may operate for the 6 remaining analyses (including four analyses containing less than 5 ppm Li) with high $[(Y + REE)/(Li + P)]_{atomic}$ (>1.7).

Slow rates of Li chemical diffusion in zircons are proven by the Li zoning in the analyzed zircons, older than 2.8 Ga, up to 4.35 Ga for Jack Hills zircons (Fig. 4). Likewise, Li tracer diffusion has been arrested as shown by the zoned δ^7Li values in zircons. Taken zircon by zircon, the average compositions of δ^7Li in cores are 10‰ different from the average compositions of rims within the TTG, sanukitoid, and Jack Hills zircons (Tables 2, 3, 4). This variation is more than five times the average standard deviation obtained for each measurement (Tables 2, 3, 4). While the existing data are not sufficiently detailed to define any possible profile due to tracer diffusion, the gradients prove that these zircons have not been homogenized.

Two of the analysis pits in TTG zircons have [Li] < 5 ppm and higher analytical uncertainties, from ±4 to ±9.9‰ (2SD). As mentioned earlier, other substitution mechanisms could be active at low concentration (e.g., [Li] < 5 ppm). Thus, zircon domains with low [Li] may have non-equilibrium δ^7Li compositions that are not representative of the melt in which the zircons formed. They are not taken into account in the following "Discussion".

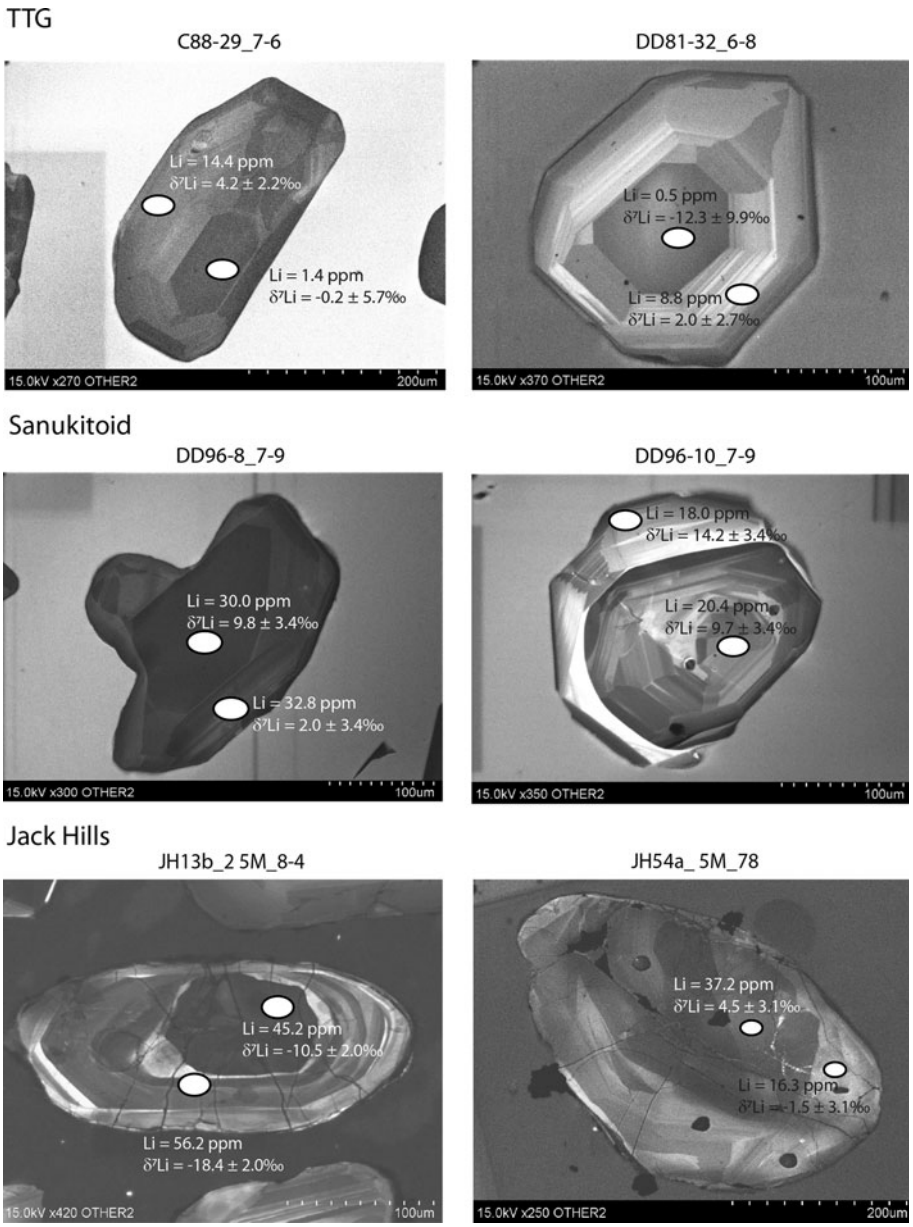

Fig. 4 CL images of the TTG, sanukitoid, and Jack Hills zircons for which two analyses in each zircon have been performed. Spot locations where both trace element abundances and Li isotope ratios were measured are shown. [Li] and δ^7Li composition of each *spot* are indicated

To summarize, the sharp Li gradients prove that intragrain chemical diffusion is slow, consistent with the link between REE and Li. Likewise, there is no evidence of Li tracer diffusion, suggesting that Li isotope exchange is also slow in zircon. Thus, [Li] and possibly δ^7Li can be used as petrogenetic tracers.

Li as petrogenetic tool: applications to Archean and Hadean zircons

Zircons from continental crust

Discrimination based on Li and other trace elements The TTG and sanukitoid plutons sampled in this study represent common components of Archean continental crust. These granitic rocks were formed from differentiated magmas (Davis et al. 2005; King et al. 1998) and this provenance is reflected by trace elements and isotope chemistry of their zircons. Grimes et al. (2007) proposed a discriminant diagram based on U/Yb ratio and Y content to distinguish between zircons from continental crust, ocean crust, and the mantle (kimberlite megacrysts). In Fig. 6, TTG and sanukitoid Type-1 zircons plot in the field of continental zircons rather than the oceanic zircon field and, more specifically, most plot in the field of continental granitoids.

Li content of zircon can also be used to discriminate between oceanic and continental crust origin. Li contents from TTGs and sanukitoids are in the range of previously reported for zircons from continental crust (Ushikubo et al. 2008) (Fig. 7). These zircons are 100–10,000 times higher

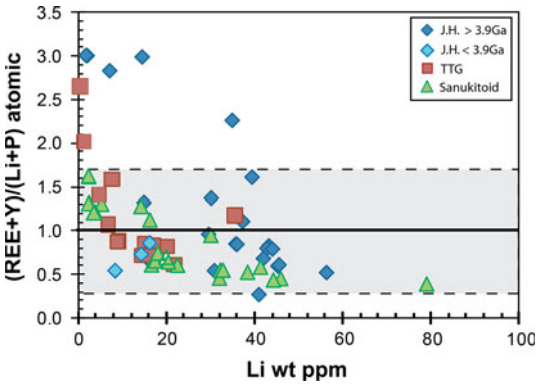

Fig. 5 (Y + REE)/(Li + P) atomic ratios versus [Li] for analyses of single 10- to 15-μm spots in Type-1 zircons. Most analyses display (Y + REE)/(Li + P) atomic ratios of 1.0 ± 0.7 (analytical uncertainty *gray box*, 2SD), consistent with the incorporation of Li on an interstitial site charge balanced by REE (see text)

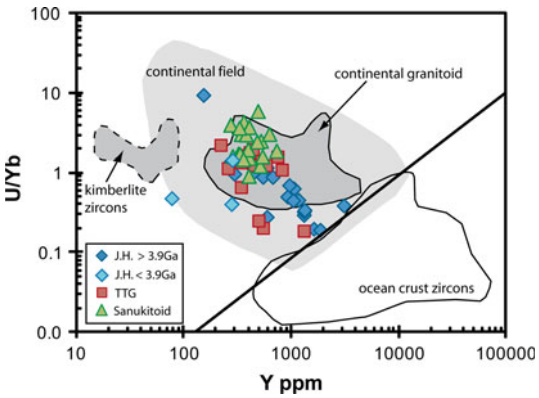

Fig. 6 U/Yb versus [Y] in zircons, modified after Grimes et al. (2007). All Type-1 zircons from this study plot in the field for continental crust. The *diagonal black line* represents the upper limit of U/Yb for zircons that are unambiguously from continental crustal. The continental field represents >1,500 analyses of Phanerozoic and Archean continental zircons (Grimes et al. 2007). The granitoid field represents zircons from northern Chile and eastern Australia (Ballard et al. 2002; Belousova et al. 2006). Zircon megacrysts from kimberlite are from Belousova et al. (1998) and Page et al. (2007)

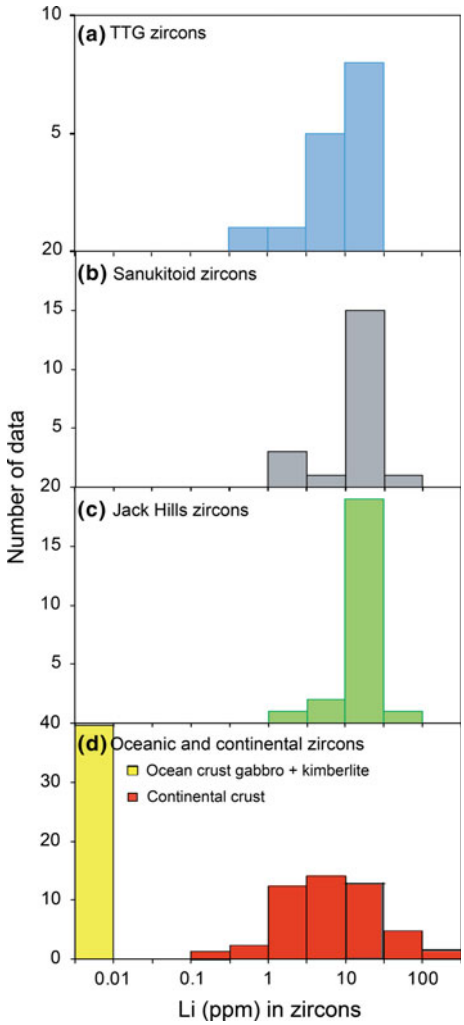

Fig. 7 Histograms of [Li] content in Type-1 zircons from TTG (**a**), sanukitoid (**b**), and Jack Hills (**c**), and a comparison of [Li] in oceanic crust and kimberlite zircons versus continental crust zircons (**d**). Zircons from oceanic crust and kimberlites are uniformly low in [Li] (<0.01 ppm), while zircons from continental crust are 100–10,000 times higher (Grimes et al. 2011; Ushikubo et al. 2008)

in [Li] than in oceanic crust zircons (Grimes et al. 2011). Thus, a bimodal distribution of Li in zircons from different tectonic settings is observed, perfectly correlating with differentiated continental versus more primitive oceanic crust and the mantle (Fig. 7).

The Li data allow the estimation of the partition coefficient between zircon and evolved melt ($D_{Li\ zircon/melt}$). While no data exist for direct comparison, and no data comparison with sanukitoid are yet published, the average [Li] in granitoid rocks with similar petrogenesis to TTG is 43 ppm (range = 2.8–179 ppm; Teng et al. 2009) when [Li] in TTG zircons average at 13.1 ppm. This ratio (13:43 or ~1:3) suggests a $D_{Li\ zircon/melt}$ of ~0.3, though the effect of variable trivalent cations (i.e., Eq. 2) is not known.

Comparison of Li isotope ratios with magma genesis models TTG and sanukitoid zircon analyses from this study are the first data set of Li isotope ratios in a suite of zircons from continental crust, allowing comparison to published whole-rock data (WR, Fig. 8). Because Li isotopes show little or no fractionation at high temperatures during partial melting (Δ^7Li(melt-rock) = 0.2–0.5‰; Jeffcoate et al. 2007) or inter-mineral equilibrium (Tomascak et al. 1999) on Earth, the primary values of δ^7Li(Zrc) should be nearly the same as the Li isotopic composition of parental rocks and magma. We thus assume that Li isotopic fractionation between melt and zircon is smaller than 2‰,

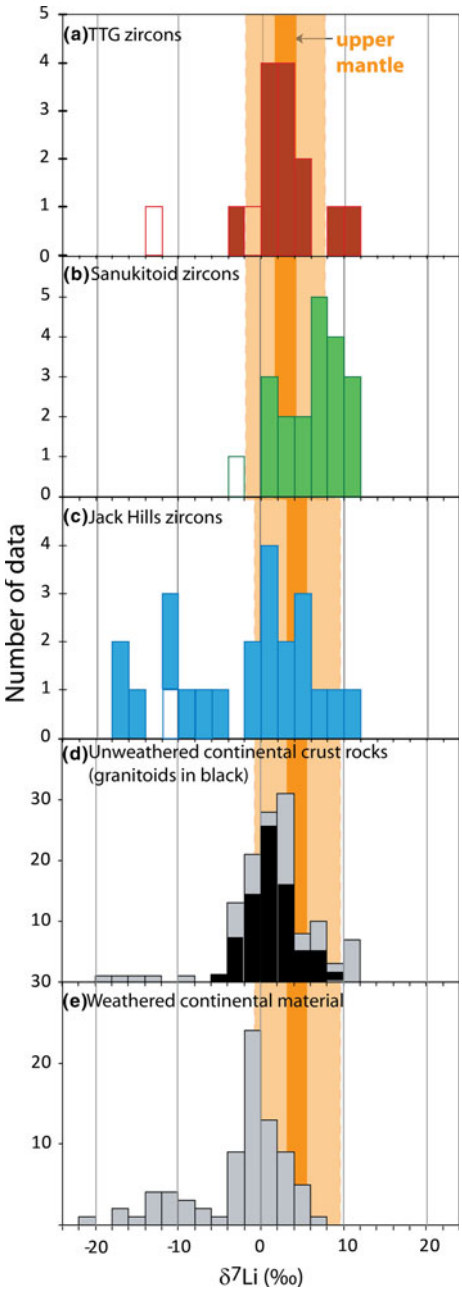

◀ **Fig. 8** Histograms of δ^7Li in TTG zircons (**a**), sanukitoid zircons (**b**) Jack Hills > 3.9-Ga zircons (**c**), and in rocks from continental crust (**d**), and weathered continental material (**e**). For comparison, average upper mantle values are plotted both without (*dark orange* band) and with analytical uncertainty for our SIMS analyses of zircon (*light orange*). The upper mantle represents the compositions of fresh peridotites and fresh N-MORB (δ^7Li = 3.8 ± 1.5‰; Chan et al. 1992; Elliott et al. 2006; Jeffcoate et al. 2007; Magna et al. 2006; Seitz et al. 2004; Tomascak et al. 2008). The range of unaltered continental rocks includes magmatic, metamorphic, and sedimentary rocks (Bryant et al. 2004; Magna et al. 2010; Marks et al. 2007; Teng et al. 2004, 2006a, b, 2008, 2009). Weathered continental rocks are from Huh et al. (2001), Kisakürek et al. (2004), Moriguti and Nakamura (1998), Rudnick et al. (2004), and Teng et al. (2004). TTG and sanukitoid zircons have similar δ^7Li values to continental rocks. Over half of Jack Hills zircons (60%) plot in the field of continental rocks, whereas 40% have lower values. *Empty boxes* represent values for zircon domains with [Li] < 5 ppm

values of the analytical uncertainties (2SD), and directly compare values of δ^7Li(Zrc) to δ^7Li(WR).

TTG zircons

TTG zircons can be compared with other granitoids and Archean TTGs (Magna et al. 2010; Teng et al. 2008, 2009). Teng et al. (2008) reported whole-rock [Li] and δ^7Li for Archean terranes, including TTGs. Archean TTG values of δ^7Li(WR) vary from 2.6 to 7.5‰, with an average of 4.1 ± 3.9‰ (2SD). Paleozoic and Mesozoic granitoids have δ^7Li(WR) from −4.5 to +8.9‰, with an average of 1.2 ± 5.5‰ (2SD) (Magna et al. 2010; Teng et al. 2009). TTG zircons (δ^7Li = 3.0 ± 7.6‰) have compositions similar to these Archean TTG and granitoid rocks, suggesting that Li isotopes in zircons are not largely altered over >2.5 Ga.

TTGs are generally thought to form from melting of either hydrated subducted tholeiitic crust or hydrous basaltic material at the base of thickened crust (e.g., Huang et al. 2010; Xiong et al. 2009). Interestingly, most TTG zircons plot in the field of mantle or primitive values when analytical uncertainty is considered (Fig. 8a). The similarity of δ^{18}O composition for TTG zircons, which averages 5.5 ± 0.4‰, and the upper mantle has also been reported for of these samples (King et al. 1998; Valley et al. 1998). The similarity of δ^7Li and δ^{18}O for TTG zircons and the upper mantle compositions are consistent with melting of weakly altered basaltic material, which could generate hydrous magmas in which zircons grow without significant shifts in δ^{18}O (Grimes et al. 2011), and Li content and isotopic composition.

Sanukitoid zircons

Sanukitoids are proposed to form by melting of metasomatized mantle-wedge peridotite, followed by fractional crystallization in the crust. The amounts of crustal contamination and composition of metasomatizing fluids (aqueous or silicate melt) are uncertain (Martin et al. 2009; Moyen et al. 1997; Shirey and Hanson 1984; Smithies and Champion 1999; Stern 1989; Stern and Hanson 1991; Stevenson et al. 1999, 2009).

Higher [Li] in sanukitoid zircons (average = 25.6 ppm) in comparison with TTG zircons (average = 13.1 ppm) is consistent with extensive fractional crystallization, commonly suggested for the sanukitoid parental melts (e.g., Stevenson et al. 1999), and the moderately incompatible

behavior of Li. No measurements of [Li] associated with δ^7Li(WR) have been taken in sanukitoid rocks to date, and thus no direct comparison between zircon and whole-rock composition is possible. The δ^7Li values of sanukitoid zircons plot near the range of unweathered rocks from continental crust (Fig. 8b, d). Sanukitoid zircons have higher δ^7Li(Zrc) values than TTG zircons and granitoid rocks, with an average of 6.8 ± 8.2‰ (2SD). A large portion of sanukitoid zircons (11 out of 16 zircons with [Li] > 5 ppm) have higher δ^7Li than the mantle. Likewise, values of δ^{18}O(Zrc) in sanukitoids (6.4 ± 0.4‰; King et al. 1998) are higher than in the mantle range. The higher δ^7Li in sanukitoid zircons compared with the mantle is consistent with the hypothesis of melting metasomatized mantle to generate the parental melts of Superior Province sanukitoids. Indeed, Marschall et al. (2007) suggested that fluids released from the slab during dehydration have δ^7Li = 10.6–23.3‰, depending on the alteration degree of the ocean crust and the depth of release. These authors modeled the Li budget of subducting oceanic crust during dehydration, based on Rayleigh distillation and taking into account that ^{7}Li is preferentially mobilized in fluids relative to ^{6}Li (Δ^7Li(mineral-fluid) < 0; e.g., Chan et al. 1993; Wunder et al. 2006). Following this model, aqueous fluids derived from the dehydration of altered oceanic crust would thus have higher δ^7Li than the mantle, and the input of dehydration fluid would increase δ^7Li of the mantle wedge. Li isotopes thus support the role of aqueous fluids as agents of metasomatism. However, metasomatism by TTG-like melts alone would not appreciably change the δ^7Li of overlying mantle. Indeed, since TTG and mantle peridotite have the same δ^7Li, metasomatism by TTG melts would not create higher δ^7Li, as is observed in sanukitoid zircons.

Application to Jack Hills zircons

The apparent retentiveness of [Li] and δ^7Li in TTG and the consistency of sanukitoid zircons and whole-rock data suggest that these characteristics can be used as petrogenetic tracers for zircons where the parent rock is not known. We thus compare Jack Hills > 3.9-Ga zircons with TTG and sanukitoid zircons, as well as with rocks from the mantle and oceanic or continental crust (Figs. 6, 7, 8) in order to restrict the origin of the detrital zircons.

Jack Hills zircons have [Li] matching the range for sanukitoid and TTG zircons (Fig. 7). The Li contents are not consistent with any zircons that have been analyzed from oceanic crust or the mantle, and indicate a differentiated magma source, such as continental-type crust. Even the oldest zircons (4.35 Ga), with [Li] = 49 ppm (Table 4), record growth in proto-continental crust. A continental-style origin is also suggested by the composition of trace elements (Fig. 6), and the values of δ^{18}O(Zrc), which average 6.2 ± 1.7‰ (2SD), higher than TTG zircons (~5.5 ± 0.8‰; King et al. 1998), but similar to sanukitoid zircons (6.4 ± 0.4‰; King et al. 1998). Most of the δ^7Li values of Jack Hills zircons (60%) are similar to those of TTGs and sanukitoids, which may also suggested similar range of parental melts.

Domains with low values of δ^7Li (<−4‰) are seen for some Jack Hills zircons but are not reported for the Archean granitoid suite. These low δ^7Li domains have the same REE patterns and similar total REE content (76–1,197 ppm, one outlier at 1,925 ppm) as Jack Hills zircons with δ^7Li > −4‰ (78–1,072 ppm). They have variable [Li], in the range of other Jack Hills zircons (Fig. 2; Table 4). Low δ^7Li values (<−4‰) have been found mostly in cores of zircons (n = 5 of 7). If magmatic, then a low δ^7Li parent rock is needed to explain observed low δ^7Li in Jack Hills zircons. As discussed by Ushikubo et al. (2008), the low values of δ^7Li(Zrc) are best matched by weathered material from continental crust (Fig. 8e). Thus, the [Li] and δ^7Li values for >3.9-Ga zircons are a good match to those from TTGs and sanukitoids with the exception of these very low Li isotope ratios in some zircons, which have been proposed to result from extensive weathering before 3.9 Ga (Ushikubo et al. 2008).

These similarities of [Li] and other trace elements, and δ^7Li and δ^{18}O, suggest that granitic rocks similar to TTG and possibly sanukitoids could both have been the parent rocks for the Jack Hills zircons.

Conclusions

We present the first data set of trace element analyses coupled to [Li] and δ^7Li in single domains of Archean zircons with known parent rocks. The new data show that:

1. Xenotime substitution alone cannot fully account for the substitution of non-tetravalent ions. The correlations between [Li] and other trace elements are consistent with the interpretation that for grains with >5 ppm, most of the Li substitutes in interstitial sites in zircon, and charge compensates for trivalent cations. However, other substitutions are possible for Li that are not charge balanced by REE (Eqs. 3 and 4), especially at low [Li] < 5 ppm.
2. Two types of REE pattern are present in the Archean zircons analyzed. Type-1 REE patterns are from domains with low Ca and concordant U–Pb age, which indicates that Type-1 zircons preserve primary magmatic compositions. Type-2 REE patterns are from domains enriched in LREE and are secondary in origin.
3. Primary Li contents and δ^7Li appear to be preserved in Type-1 zircons with >5 ppm Li. Different compositions

of cores and rims in zircons do not support fast chemical diffusion of Li, which would have homogenized the observed Li gradients. Relatively slow chemical diffusion of Li and preservation of magmatic [Li] are supported by the coupled interstitial substitution of Li and REE (Eq. 2), because REE are known to have slow diffusion rates in zircon. Zoned zircons further suggest that Li isotope exchange by tracer diffusion has not affected the analyzed zircons.

4. Li contents in the analyzed TTG and sanukitoid zircons are similar to published values for zircons from continental crust but are distinct from zircons in oceanic crust or mantle megacrysts from kimberlite. Thus, [Li] > 0.1 ppm in is an index for differentiated magmas in continental crust. [Li] in TTG is consistent with growth in a granitoid melt, and the higher [Li] in sanukitoid zircons agrees with extensive fractional crystallization proposed for these rocks.
5. TTG and sanukitoid zircons have δ^7Li values that span the range of unweathered continental crust. TTG zircons have δ^7Li and δ^{18}O similar to pristine magmas from the mantle, consistent with parent magma formed by melting of basaltic material. Sanukitoid zircons have a slightly higher average δ^7Li than the mantle and TTGs, in agreement with parental magma generated by melting of fluid-metasomatized mantle. The present results thus indicate that Archean zircons with igneous signature (Type-I REE pattern and low Ca concentration) preserve primordial Li compositions.
6. The high [Li] in Jack Hills zircons (6–71 ppm) and other trace elements suggest that they grew in granitoids of proto-continental crust. Most of the Jack Hills zircons have δ^7Li and δ^{18}O similar to those of TTG and sanukitoid zircons, consistent with the proposal that these rocks were protoliths for many of the detrital zircons, as also suggested by [Ti]. A subset of Jack Hills zircons have extremely low δ^7Li (-18 to -4‰), reflecting melting of extensively weathered crust.

Acknowledgments The authors thank Jim Kern for maintaining the ion microprobe, John Fournelle for assistance on the SEM, and Brian Hess for expertise in sample preparation. Don Davis and Elizabeth King are thanked for zircon separates from their studies. This study was funded by NSF-EAR (0838058) and DOE (93ER14389). The WiscSIMS Lab is partially funded by NSF-EAR (0319230, 0516725, 0744079, and 1053466).

References

Aines RD, Rossman GR (1986) Relationships between radiation damage and trace water in zircon, quartz, and topaz. Am Mineral 71(9–10):1186–1193

Ballard J, Palin M, Campbell I (2002) Relative oxidation states of magmas inferred from Ce(IV)/Ce(III) in zircon: application to porphyry copper deposits of northern Chile. Contrib Mineral Petrol 144(3):347–364. doi:10.1007/s00410-002-0402-5

Barker F (1979) Trondhjemite: definition, environment and hypotheses of origin. In: Barker F (ed) Trondhjemites, dacites and related rocks. Elsevier, Amsterdam, pp 1–12

Barth AP, Wooden JL (2010) Coupled elemental and isotopic analyses of polygenetic zircons from granitic rocks by ion microprobe, with implications for melt evolution and the sources of granitic magmas. Chem Geol 277(1–2):149–159

Beakhouse GP, McNutt RH (1991) Contrasting types of Late Archean plutonic rocks in northwestern Ontario: implications for crustal evolution in the Superior Province. Precambrian Res 49:141–165

Belousova EA, Griffin WL, Pearson NJ (1998) Trace element composition and cathodoluminescence properties of southern African kimberlitic zircons. Mineral Mag 62:355–366

Belousova EA, Griffin WL, O'Reilly SY (2006) Zircon crystal morphology, trace element signatures and Hf isotope composition as a tool for petrogenetic modelling: examples from Eastern Australian granitoids. J Petrol 47(2):329–353. doi:10.1093/petrology/egi077

Bowman JR, Moser DE, Valley JW, Kita NT, Mazdab F (2011) U-Pb age, δ^{18}O and trace element zoning in deep crustal zircon from the Kapuskasing Uplift; guidelines for interpreting Archean zircon records of high temperature crustal evolution and lithosphere-fluid interactions. Contr Min Pet (accepted)

Bryant CJ, Chappell BW, Bennett VC, McCulloch MT (2004) Lithium isotopic compositions of the New England Batholith: correlations with inferred source rock compositions. Earth Env Sci Trans R Soc Edinb 95(1–2):199–214. doi:10.1017/S0263593300001012

Caruba R, Iacconi P (1983) Les zircons des pegmatites de Narssârssuk (Groënland) — L'eau et les groupements OH dans les zircons métamictes. Chem Geol 38(1–2):75–92. doi:10.1016/0009-2541(83)90046-3

Cavosie AJ, Wilde SA, Liu D, Weiblen PW, Valley JW (2004) Internal zoning and U-Th-Pb chemistry of Jack Hills detrital zircons: a mineral record of early Archean to Mesoproterozoic (4348–1576 Ma) magmatism. Precambrian Res 135:251–279

Cavosie AJ, Valley JW, Wilde SA, EIMF (2005) Magmatic δ^{18}O in 4400–3900 Ma detrital zircons: a record of the alteration and recycling of crust in the Early Archean. Earth Planet Sci Lett 235:663–681

Cavosie AJ, Valley JW, Wilde SA, EIMF (2006) Correlated microanalysis of zircon: Trace element, δ^{18}O, and U-Th-Pb isotopic constraints on the igneous origin of complex > 3900 Ma detrital grains. Geochim Cosmochim Acta 70:5601–5616

Cavosie AJ, Kita NT, Valley JW (2009) Primitive oxygen-isotope ratio recorded in magmatic zircon from the Mid-Atlantic Ridge. Am Mineral 94(7):926–934. doi:10.2138/am.2009.2982

Chan L-H, Edmond JM (1988) Variation of lithium isotope composition in the marine environment: a preliminary report. Geochim Cosmochim Acta 52:1711–1717

Chan LH, Edmond JM, Thompson G, Gillis K (1992) Lithium isotopic composition of submarine basalts: implications for the lithium cycle in the oceans. Earth Planet Sci Lett 108:151–160

Chan L-H, Edmond JM, Thompson G (1993) A lithium isotope study of hot springs and metabasalts from mid-ocean ridge hydrothermal systems. J Geophys Res 98. doi:10.1029/92jb00840

Chan L-H, Alt JC, Teagle DAH (2002a) Lithium and lithium isotope profiles through the upper oceanic crust: a study of seawater-basalt exchange at ODP Sites 504B and 896A. Earth Planet Sci Lett 201(1):187–201

Chan LH, Leeman WP, You CF (2002b) Lithium isotopic composition of Central American volcanic arc lavas: implications for modification of subarc mantle by slab-derived fluids: correction. Chem Geol 182:293–300

Cherniak DJ, Watson EB (2003) Diffusion in zircon. In: Hanchar JM, Hoskin WO (eds) Zircon, vol Rev Min Geoch, pp 113–139
Cherniak D, Watson E (2010) Li diffusion in zircon. Contrib Mineral Petrol 160(3):383–390. doi:10.1007/s00410-009-0483-5
Cherniak DJ, Hanchar JM, Watson EB (1997) Rare-earth diffusion in zircon. Chem Geol 134:289–301
Condie K (2005) TTGs and adakites: are they both slab melts? Lithos 80:33–44
Crowley JL, Myers JS, Sylvester PJ, Cox RA (2005) Detrital zircon from the Jack Hills and Mount Narryer, Western Australia: evidence for diverse 14.0 Ga source rocks. J Geol 113:239–263
Davis WD, Williams IS, Krogh TE (2003) Historical development of zircon geochronology. In: Hanchar JM, Hoskin PWO (eds) Zircon, vol Rev Min Geoch, pp 145–182
Davis DW, Amelin Y, Nowell GM, Parrish RR (2005) Hf isotopes in zircon from the western Superior Province, Canada: Implication for the Archean crustal development and evolution of the depleted mantle reservoir. Precambrian Res 140:132–156
Dohmen R, Kasemann SA, Coogan L, Chakraborty S (2010) Diffusion of Li in olivine. Part I: experimental observations and a multi species diffusion model. Geochim Cosmochim Acta 74(1):274–292
Drummond MS, Defant MJ (1990) A model for trondhjemite-tonalite-dacite genesis and crustal growth via slab melting: Archean to modern comparisons. J Geophys Res 95:21503–21521
Elliott T, Thomas A, Jeffcoate A, Niu Y (2006) Lithium isotope evidence for subduction-enriched mantle in the source of mid-ocean-ridge basalts. Nature 443(7111):565–568. doi:http://www.nature.com/nature/journal/v443/n7111/suppinfo/nature05144_S1.html
Ferry J, Watson E (2007) New thermodynamic models and revised calibrations for the Ti-in-zircon and Zr-in-rutile thermometers. Contrib Mineral Petrol 154(4):429–437. doi:10.1007/s00410-007-0201-0
Finch JR, Hanchar JM, Hoskin PWO, Burns PC (2001) Rare-earth elements in synthetic zircon: part 2. A single crystal X-ray study of xenotime substitution. Am Mineral 86:681–689
Frondel C (1953) Hydroxyl substitution in thorite and zircon.
Fu B, Page F, Cavosie A, Fournelle J, Kita N, Lackey J, Wilde S, Valley J (2008) Ti-in-zircon thermometry: applications and limitations. Contrib Mineral Petrol 156(2):197–215. doi:10.1007/s00410-008-0281-5
Geisler T, Schleicher H (2000a) Improved U-Th-total Pb dating of zircons by electron microprobe using a new background modeling method and Ca as a chemical indicator of fluid-induced U-Th-Pb discordance in zircon. Chem Geol 163:269–285
Geisler T, Schleicher H (2000b) Improved U-Th-total Pb dating of zircons by electron microprobe using a simple new background modeling procedure and Ca as a chemical criterion of fluid-induced U-Th-Pb discordance in zircon. Chem Geol 163(1–4):269–285
Geisler T, Pidgeon RT, Kurtz R, Van Bronswijk W, Schleicher H (2003a) Experimental hydrothermal alteration of partially metamict zircon. Am Mineral 88:1496–1513
Geisler T, Rashwan AA, Rahn M, Poller U, Zwingmann H, Pidgeon RT, Schleicher H (2003b) Low-temperature hydrothermal alteration of natural metamict zircons from the Eastern Desert, Egypt. Mineral Mag 67:485–508
Grimes CB, John BE, Kelemen PB, Mazdab FK, Wooden JL, Cheadle MJ, Hanghøj K, Schwartz JJ (2007) Trace element chemistry of zircons from oceanic crust: a method for distinguishing detrital zircon provenance. Geology 35(7):643–646. doi:10.1130/g23603a.1
Grimes C, John B, Cheadle M, Mazdab F, Wooden J, Swapp S, Schwartz J (2009) On the occurrence, trace element geochemistry, and crystallization history of zircon from in situ ocean lithosphere. Contrib Mineral Petrol 158(6):757–783. doi:10.1007/s00410-009-0409-2
Grimes C, Ushikubo T, John B, Valley JW (2011) Uniformly mantle-like $\delta^{18}O$ in zircons from oceanic plagiogranites and gabbros. Contrib Mineral Petrol 161(1):13–33. doi:10.1007/s00410-010-0519-x
Halden NM, Hawthorne FC, Campbell JL, Teesdale WJ, Maxwell JA, Higuchi D (1993) Chemical characterization of oscillatory zoning and overgrowths in zircon using 3 MeV μ-PIXE. Can Mineral 31:637–647
Hanchar JM, Finch JR, Hoskin PWO, Watson EB, Cherniak DJ, Mariano AN (2001) Rare earth element in synthetic zircon. Part 1: synthesis, and rare earth element and phosphorus doping. Am Mineral 86:667–680
Harrison TM, Schmitt AK (2007) High sensitivity mapping of Ti distributions in Hadean zircons. Earth Planet Sci Lett 261(1–2):9–19
Hinton RW, Upton BGJ (1991) The chemistry of zircon: variations within and between large crystals from syenite and alkali basalt xenoliths. Geochim Cosmochim Acta 55:3287–3302
Hoskin PWO (2005) Trace-element composition of hydrothermal zircon and the alteration of Hadean zircon from the Jack Hills, Australia. Geochim Cosmochim Acta 69:637–648
Hoskin PWO, Schaltegger U (2003) The composition of zircon and igneous and metamorphic petrogenesis. In: Hanchar JM, Hoskin PWO (eds) Zircon, vol 53. Rev Min Geoch, pp 27–55
Hoskin PWO, Kinny PD, Wyborn D, Chappell BW (2000) Identifying accessory mineral saturation during differentiation in granitoid magmas: an interpreted approach. J Petrol 41:1365–1396
Huang X-L, Niu Y, Xu Y-G, Yang Q-J, Zhong J-W (2010) Geochemistry of TTG and TTG-like gneisses from Lushan-Taihua complex in the southern North China Craton: implications for late Archean crustal accretion. Precambrian Res 182(1–2):43–56
Huh Y, Chan L-H, Edmond JM (2001) Lithium isotopes as a probe of weathering processes: Orinoco River. Earth Planet Sci Lett 194(1–2):189–199
Jeffcoate AB, Elliott T, Kasemann SA, Ionov D, Cooper K, Brooker R (2007) Li isotope fractionation in peridotites and mafic melts. Geochim Cosmochim Acta 71:202–218
Kasemann S, Jeffcoate A, Elliott T (2005) Lithium isotope composition of basalt glass reference material. Anal Chem 77:5251–5257
King EM, Valley JW, Davis DW, Edwards GR (1998) Oxygen isotope ratios of Archean plutonic zircons from granite-greenstone belts of the Superior Province: indicator of magmatic source. Precambrian Res 92:365–387
Kisakürek B, Widdowson M, James RH (2004) Behaviour of Li isotopes during continental weathering: the Bidar laterite profile, India. Chem Geol 212(1–2):27–44
Lancaster PJ, Fu B, Page FZ, Kita NT, Bickford ME, Hill BM, McLelland JM, Valley JW (2009) Genesis of metapelitic migmatites in the Adirondack Mts., New York. J Meta Geol 27:41–54
Li X-H, Li Q-L, Liu Y, Tang G-Q (2011) Further characterization of M257 zircon standard: a working reference for SIMS analysis of Li isotopes. J Anal At Spectrom 26(2):352–358
Lundstrom CC, Chaussidon M, Hsui AT, Kelemen P, Zimmerman M (2005) Observations of Li isotopic variations in the Trinity Ophiolite: evidence for isotopic fractionation by diffusion during mantle melting. Geochim Cosmochim Acta 69:735–751
Maas R, Kinny PD, Williams IS, Froude DO, Compston W (1992) The Earth's oldest known crust: a geochronological and geochemical study of 3900–4200 Ma old detrital zircons from Mt. Narryer and Jack Hills, Western Australia. Geochim Cosmochim Acta 56:1281–1300
Magna T, Wiechert U, Halliday AN (2006) New constraints on the lithium isotope compositions of the Moon and terrestrial planets. Earth Planet Sci Lett 243(3–4):336–353. doi:10.1016/j.epsl.2006.01.005

Magna T, Janousek V, Kohút M, Oberli F, Wiechert U (2010) Fingerprinting sources of orogenic plutonic rocks from Variscan belt with lithium isotopes and possible link to subduction-related origin of some A-type granites. Chem Geol 274(1–2):94–107

Marks MAW, Rudnick RL, McCammon C, Vennemann T, Markl G (2007) Arrested kinetic Li isotope fractionation at the margin of the Ilímaussaq complex, South Greenland: evidence for open-system processes during final cooling of peralkaline igneous rocks. Chem Geol 246(3–4):207–230. doi:10.1016/j.chemgeo.2007.10.001

Marschall H, Pogge von Strandmann PAE, Seitz H-M, Elliott T, Niu Y (2007) The lithium isotopic composition of orogenic eclogites and deep subducted slabs. Earth Planet Sci Lett 262(3–4):563–580

Martin H, Smithies RH, Rapp R, Moyen J-F, Champion D (2005) An overview of adakite, tonalite-trondhjemite-granodiorite (TTG), and sanukitoid: relationships and some implications fro crustal evolution. Lithos 79:1–24

Martin H, Moyen J-F, Rapp R (2009) The sanukitoid series: magmatism at the Archaean/Proterozoic transition. Earth Environ Sci Trans R Soc Edinb 100(Special Issue 1–2):15–33. doi:10.1017/S1755691009016120

McDonough WF, Sun SS (1995) The composition of the Earth. Chem Geol 120:223–253

Millot R, Guerrot C, Vigier N (2004) Accurate and high-precision measurement of lithium isotopes in two reference materials by MC-ICP-MS. Geostand Geoanal Res 28(1):153–159. doi:10.1111/j.1751-908X.2004.tb01052.x

Moriguti T, Nakamura E (1998) Across-arc variation of Li isotopes in lavas and implications for crust/mantle recycling at subduction zones. Earth Planet Sci Lett 163(1–4):167–174

Moyen J-F, Martin H, Jayananda M (1997) Origine du granite fini-Archéen de Closepet (Inde du Sud): apports de la modélisation géochimique du comportement des éléments en traces. C R Acad Sci Paris 325:659–664

Murakami T, Chakoumakos BC, Ewing RC, Lumpkin GR, Weber WJ (1991) Alpha-decay damage in zircon. Am Mineral 76:1510–1532

Page FZ, Fu B, Kita NT, Fournelle J, Spicuzza MJ, Schulze DJ, Viljoen V, Basei MAS, Valley JW (2007) Zircons from kimberlites: new insights from oxygen isotopes, trace elements, and Ti in zircon thermometry. Geochim Cosmochim Acta 71:3887–3903

Pearce NJG, Westgate JA, Perkins WT (1996) Developments in the analysis of volcanic glass shards by laser ablation ICP-MS: quantitative and single internal standard-multielement methods. Quat Int 34–36:213–227

Pearce NJ, Perkins WT, Westgate JA, Gorton MP, Jackson SE, Neal CR, Chenery SP (1997) A compilation of new and published major and trace element data for NIST SRM 610 and NIST SRM 612 glass reference material. Geostand Newslett 21:115–144

Peck WH, Valley JW, Wilde SA, Graham CM (2001) Oxygen isotope ratios and rare earth elements in 3.3 to 4.4 Ga zircons: Ion microprobe evidence for high $\delta^{18}O$ continental crust and oceans in the Early Archean. Geochim Cosmochim Acta 65:4215–4229

Pidgeon RT, Nemchin AA, Hitchen GJ (1998) Internal structures of zircons from Archean granites from the Darling Range batholith: implications for zircon stability and the interpretation of zircon U-Pb ages. Contrib Mineral Petrol 132:288–299

Pistiner JS, Henderson GM (2003) Lithium-isotope fractionation during continental weathering processes. Earth Planet Sci Lett 214:327–339

Rayner N, Stern RA, Carr SD (2005) Grain-scale variations in trace element composition of fluid-altered zircon, Acasta Gneiss Complex, northwestern Canada. Contrib Mineral Petrol 148(6):721–734

Richter FM, Davis AM, DePaolo DJ, Watson EB (2003) Isotope fractionation by chemical diffusion between molten basalt and rhyolite. Geochim Cosmochim Acta 67:3905–3923

Romans PA, Brown LL, White JC (1975) An electron microprobe study of yttrium, rare earth, and phosphorus distribution in zoned and ordinary zircons. Am Mineral 60:475–480

Rudnick RL, Ionov DA (2007) Lithium elemental and isotopic disequilibrium in minerals from peridotite xenoliths from far-east Russia: product of recent melt/fluid–rock reaction. Earth Planet Sci Lett 256:278–293

Rudnick RL, Tomascak PB, Njo HB, Gardner LR (2004) Extreme lithium isotopic fractionation during continental weathering revealed in saprolites from South Carolina. Chem Geol 212:45–57

Seitz H-M, Brey GP, Lahaye Y, Durali S, Weyer S (2004) Lithium isotopic signatures of peridotite xenoliths and isotopic fractionation at high temperature between olivine and pyroxenes. Chem Geol 212(1–2):163–177. doi:10.1016/j.chemgeo.2004.08.009

Seyfried WE Jr, Chen X, Chan L-H (1998) Trace element mobility and lithium isotope exchange during hydrothermal alteration of seafloor weathered basalt: an experimental study at 350°C, 500 bars. Geochim Cosmochim Acta 62(6):949–960

Shannon RD (1976) Revised effective ionic radii and systematic studies of interatomic distances in halides and chalcogenides. Acta Cryst A32:751–767

Shirey SB, Hanson GN (1984) Mantle-derived Archean monzodiorites and trachyandesites. Nature 310:222–224

Silver LT, Deutsch S (1963) Uranium-lead isotopic variations in zircons: a case study. J Geol 71:721–758

Smithies RH (2000) The Archean tonalite-trondhjemite-granodiorite (TTG) series is not an analogue of Cenozoic adakite. Earth Planet Sci Lett 182:115–125

Smithies RH, Champion DC (1999) High-Mg diorite from the Archaean Pilbara Craton: anorogenic magmas derived from a subduction-modified mantle. Geol Surv West Aust Annu Rev 1998–1999:45–59

Speer JA (1982) Zircon. In: Orthosilicates, vol 5. Rev Min, pp 67–112

Stern RA (1989) Petrogenesis of the Archaean sanukitoid suite. State University, Stony Brook

Stern RA, Hanson GN (1991) Archean high-Mg granodiorite: a derivative of light rare earth element-enriched monzodiorite of mantle origin. J Petrol 32:201–238

Stevenson R, Henry P, Gariépy C (1999) Assimilation–fractional crystallization origin of Archean Sanukitoid Suites: Western Superior Province, Canada. Precambrian Res 96:83–99

Stevenson RK, Henry P, Gariépy C (2009) Isotopic and geochemical evidence for differentiation and crustal contamination from granitoids of the Berens river subprovince, Superior Province, Canada. Precambrian Res 168(1–2):123–133

Teng F-Z, McDonough WF, Rudnick RL, Dalpé C, Tomascak PB, Chappell BW, Gao S (2004) Lithium isotopic composition and concentration of the upper continental crust. Geochim Cosmochim Acta 68:4167–4178

Teng F-Z, McDonough WF, Rudnick RL, Walker RJ (2006a) Diffusion-driven extreme lithium isotopic fractionation in country rocks of the Tin Mountain pegmatite. Earth Planet Sci Lett 243(3–4):701–710

Teng F-Z, McDonough WF, Rudnick RL, Walker RJ, Sirbescu M-LC (2006b) Lithium isotopic systematics of granites and pegmatites from the Black Hills, South Dakota. Am Mineral 91(10):1488–1498. doi:10.2138/am.2006.2083

Teng F-Z, Rudnick RL, McDonough WF, Gao S, Tomascak PB, Liu Y (2008) Lithium isotopic composition and concentration of the deep continental crust. Chem Geol 255:47–59

Teng F-Z, Rudnick RL, McDonough WF, Wu F-Y (2009) Lithium isotopic systematics of A-type granites and their mafic enclaves:

further constraints on the Li isotopic composition of the continental crust. Chem Geol 262(3–4):370–379
Tomascak PB (2004) Developments in the understanding and application of lithium isotopes in the earth and planetary sciences. Rev Mineral Geochem 55(1):153–195. doi:10.2138/gsrmg.55.1.153
Tomascak PB, Tera F, Helz RT, Walker RJ (1999) The absence of lithium isotope fractionation during basalt differentiation: new measurements by multicollector sector ICP-MS. Geochim Cosmochim Acta 63(6):907–910
Tomascak PB, Langmuir CH, le Roux PJ, Shirey SB (2008) Lithium isotopes in global mid-ocean ridge basalts. Geochim Cosmochim Acta 72(6):1626–1637
Trail D, Mojzsis SJ, Harrison TM, Schmitt AK, Watson EB, Young ED (2007) Constraints on Hadean zircon protoliths from oxygen isotopes, Ti-thermometry, and rare earth elements. Geochem Geophys Geosyst 8. doi:10.1029/2006gc001449
Ushikubo T, Kita NT, Cavosie AJ, Wilde SA, Rudnick RL, Valley JW (2008) Lithium in Jack Hills zircons: evidence for extensive weathering of Earth's earliest crust. Earth Planet Sci Lett 272:666–676
Utsunomiya S, Valley JW, Cavosie AJ, Wilde SA, Ewing RC (2007) Radiation damage and alteration of zircon from a 3.3 Ga porphyritic granite from the Jack Hills, Western Australia. Chem Geol 236(1–2):92–111
Valley JW (2003) Oxygen isotopes in zircon. Rev Mineral Geochem 53(1):343–385. doi:10.2113/0530343
Valley JW, Kinny PD, Schulze DJ, Spicuzza MJ (1998) Zircon megacrysts from kimberlite: oxygen isotope variability among mantle melts. Contrib Mineral Petrol 133:1–11
Valley JW, Lackey J-S, Cavosie AJ, Clechenko C, Spicuzza MJ, Basei M, Bindeman I, Ferreira V, Sial AN, King E, Peck WH, Sinha A, Wei C (2005) 4.4 billion years of crustal maturation: oxygen isotope ratios of magmatic zircon. Contrib Mineral Petrol 150(6):561–580. doi:10.1007/s00410-005-0025-8
Watson EB, Baxter EF (2007) Diffusion in solid-Earth systems. Earth Planet Sci Lett 253(3–4):307–327
Watson EB, Cherniak DJ (1997) Oxygen diffusion in zircon. Earth Planet Sci Lett 148(3–4):527–544
Whitehouse MJ, Kamber BS (2003) A rare earth element study of complex zircons from early Archaean Amîtsoq gneisses, Godthåbsfjord, south-west Greenland. Precambrian Res 126:363–377
Wiedenbeck M, Hanchar JM, Peck WH, Sylvester P, Valley JW, Whitehouse MJ et al (2004) Further characterization of the 91500 zircon crystal. Geostandards Geoanalytical Res 28:9–39
Wilde SA, Valley JW, Peck WH, Graham CM (2001) Evidence from detrital zircons for the existence of continental crust and oceans on the Earth 4.4 Gyr ago. Nature 409(6817):175–178
Williams HR, Stott GM, Thurston PC, Sutcliffe RH, Bennett G, Easton RM, Armstrong DK (1991) Tectonic evolution of Ontario: summary and synthesis. In: Geology of ontario, vol Special Volume 4 part 2. Ontario Geological Survey, Ontario, Canada, pp 1255–1332
Woodhead JA, Rossman GR, Silver LT (1991) The metamictization of zircon; radiation dose-dependent structural characteristics. Am Mineral 76(1–2):74–82
Wunder B, Meixner A, Romer RL, Heinrich W (2006) T-dependent isotopic fractionation of lithium between clinopyroxene and high-pressure hydrous fluids. Contrib Mineral Petrol 151:112–120
Xiong X, Keppler H, Audetat A, Gudfinnsson G, Sun W, Song M, Xiao W, Yuan L (2009) Experimental constraints on rutile saturation during partial melting of metabasalt at the amphibolite to eclogite transition, with applications to TTG genesis. Am Mineral 94(8–9):1175–1186. doi:10.2138/am.2009.3158
You CF, Chan LH (1996) Precise determination of lithium isotopic composition in low concentration natural samples. Geochim Cosmochim Acta 60:909–915
Zhang XY, Cherniak DJ, Watson EB (2006) Oxygen diffusion in titanite: lattice diffusion and fast-path diffusion in single crystals. Chem Geol 235(1–2):105–123